Materials Today Communications 58 (2027) 116684

Contents lists available at ScienceDirect

Materials Today Communications

journal homepage: www.elsevier.com/locate/mtcomm

Physical, mechanical, and thermal characterization of Curauá (*Ananas comosus var. Erectifolius*) and carbon fiber-reinforced polymer composites for sustainable applications

Karthick Rasu [a], Arnas Majumder [b,*], Flavio Stochino [b]

[a] Department of Mechanical Engineering, Velammal College of Engineering and Technology, Madurai, Tamil Nadu 625 009, India
[b] Department of Civil Environmental Engineering and Architecture, University of Cagliari, via Marengo 2, Cagliari, CA 09123, Italy

ARTICLE INFO

Key words:
Curauá fiber
Natural fiber
Carbon fiber
Hybrid fiber
Polyester
Physical properties
Mechanical properties
Thermal properties

ABSTRACT

The development of sustainable fiber-reinforced polymer composites requires an appropriate balance between mechanical performance, moisture resistance, and thermal stability. This research explores the effect of the proportions of Curauá and carbon fiber on the physical, mechanical, thermal, and microstructural behavior of composites based on polyester. Five specimens of different fiber weight ratios in the composite but with a fixed 60% by weight polyester matrix were made by hand lay-up and compression molding. The specimens were tested for their properties by mechanical tests, water absorption test, thermogravimetric analysis (TGA) and scanning electron microscopy (SEM). Among all the studied samples, the combination Cu25-Ca15-Po60 (25 wt% Curauá fiber, 15 wt% carbon fiber, and 60 wt% polyester) showed better mechanical properties, with increases in hardness by 40.92%, tensile strength by 110.05%, flexural strength by 66.78%, and shear strength by 128.65% compared to the sample made of Curauá fibers only (Cu40-Po60). Its impact strength was 100.20% higher than that of the carbon-only composite (Ca40-Po60). The optimized hybrid composite showed 67.07% less water absorption after 24 h when compared with Cu40-Po60; the water absorption decreased from 8.2% to 2.7%; however, the Ca40-Po60 showed the minimum water absorption of 1.6%. Calculation based on five normalized mechanical properties was done by means of the Integrated Performance Index (IPI), ranking Cu25-Ca15-Po60 highest (IPI = 1.0000). SEM revealed improved interfacial bonding between fibers and matrix, along with fewer defects, while TGA indicated the hybrid system's thermal stability. From these results, it is evident that proper incorporation of Curauá-carbon fiber mixture would improve the mechanical and water-resistant properties of polyester composites and make it suitable for engineering applications.

1. Introduction

Growing awareness regarding the environment, along with an increase in carbon footprint and exhaustion of natural resources, has prompted research on the development of sustainable alternatives [1–6]. Natural fiber-reinforced polymer composites have received considerable attention because of their low density, renewability, cost-effectiveness, and potential to reduce dependence on synthetic reinforcements [7–15]. Natural fibers such as jute [16], flax [17], hemp [18], Curauá [19], banana [20], coir [21] and sisal [22] have demonstrated potential for lightweight engineering applications owing to their favorable specific mechanical properties [23]. Their utilization is also consistent with broader efforts to improve resource efficiency and promote circular-economy approaches in material development [24–27].

Notably, Curauá fiber has attracted attention because of its relatively high specific strength, low density, and renewable origin [28]. However, the mechanical performance and durability of natural fiber-reinforced composites are influenced by moisture sensitivity, fiber–matrix adhesion, reinforcement orientation, and processing conditions [29,30]. Carbon fiber has high strength and stiffness, and therefore its combination with Curauá fiber can be a good technique to make hybrid polymer composites. It can also be an effective method of balancing mechanical properties with partial replacement of synthetic reinforcement, depending on the proportion of fibers used in the composite.

It is worth to highlight, previous studies have demonstrated that the

* Corresponding author.
E-mail address: arnas.majumder@unica.it (A. Majumder).

https://doi.org/10.1016/j.mtcomm.2026.116684
Received 8 September 2026; Received in revised form 2 November 2026; Accepted 17 November 2026
Available online 19 November 2026
2352-4928/© 2026 The Author(s). Published by Elsevier Ltd. This is an open access article under the CC BY license (http://creativecommons.org/licenses/by/4.0/).

mechanical performance of Curauá-based composites depends strongly on fiber architecture, reinforcement content, processing conditions, and interfacial adhesion [19] [28] [29 [31]. Sharma et al. [32] reported that polypropylene composites containing 18 wt% alkali-treated Curauá fibers achieved tensile and flexural strengths of 67 ± 2 MPa and 79 ± 1 MPa, respectively, with an interfacial strength of 9.8 ± 0.1 MPa. Araujo et al. [29 identified 20 wt% Curauá fibers and 2 wt% coupling agent as a favorable formulation for improving interfacial compatibility and reducing moisture sensitivity.

Further it can be found that the hybridization and surface modification have also produced notable improvements. Minillo et al. [33] investigated Curauá/glass fiber-reinforced epoxy composites for nautical applications through numerical modeling. Premkumar et al. [34] reported that basalt hybridization increased the temperature associated with approximately 2% mass loss from 150 to 190 °C, representing a 40 °C improvement in the investigated Curauá/polyester system. Costa et al. [35] demonstrated that graphene oxide (GO) functionalization of the epoxy matrix increased the yield strength by 64%, tensile strength by 40%, Young's modulus by 60%, and toughness by 28% relative to unmodified Curauá/epoxy composites. Whereas other studies on Curauá/glass and Curauá/aramid composites highlighted the importance of fiber arrangement and interfacial behavior, although partial replacement of synthetic fibers did not consistently improve all mechanical properties [33–44].

Recent investigations have confirmed the benefits of surface engineering in other natural-fiber composites. Islam et al. [45] reported approximately 113% higher tensile strength and 93% higher flexural strength for alkali-treated and GO-coated bamboo/epoxy composites compared with untreated composites. Similarly, Islam et al. [46] developed GO-modified jute/glass hybrid composites using fiber wrapping, achieving a tensile strength of 272.63 MPa, flexural modulus of 10.42 GPa, impact resistance of 85.56 kJ/m^2, and water absorption of 1.12%. Hossain et al. [47] further reviewed the potential of nanotechnology-assisted textile functionalization for improving material performance. In other cases, the sustainability potential of natural-fiber composites has also been demonstrated. Notably, Wasti et al. [26] reported approximately 34–40% lower cradle-to-gate energy demand and greenhouse gas emissions for coir/polypropylene automotive components compared with glass-fiber/polypropylene alternatives. Limwibul et al. [30] reported carbon-footprint reductions of up to 88.6% for the investigated natural-fiber/bioresin composites. However, these environmental benefits are specific to the materials and assessment conditions considered. Hybrid composites have also been explored for lightweight and structural engineering applications [48–51].

The novelty of the present study lies in the systematic investigation of Curauá–carbon fiber hybridization in polyester-based composites. Particular emphasis has been placed on identifying the influence of reinforcement proportions on overall performance. While prior studies mostly focused on the development of alternative fiber hybrids or specific material characteristics [33–44]. Whereas this study uses a combination of mechanical, physical, thermal, and microstructural evaluations with an Integrated Performance Index (IPI) for a complete analysis of composite behavior.

2. Materials and methods

The experimental methodology was specifically formulated to systematically investigate the effect of Curauá/carbon fiber composite on the properties of polyester-based composites. Five composite formulations were developed by varying the Curauá-to-carbon fiber ratio while maintaining constant total fiber (40 wt%) and polyester matrix (60 wt%) contents. Mechanical testing, water absorption measurements, thermogravimetric analysis (TGA), and scanning electron microscopy (SEM) were employed to characterize composite performance. Moreover, statistical analysis, including ANOVA, was carried out to investigate any differences in the mechanical properties of the formulations, and IPI was used to determine the formulation with the best composition in terms of mechanical performance characteristics. The presented experimental approach draws a clear link between the research objectives and performance evaluation.

2.1. Materials

The hybrid composite developed in this study consists mainly of Curauá fiber, carbon fiber, and a polyester resin matrix.

Fig. 1(a) represents the Curauá plant, which belongs to the species Ananas erectifolius, and the raw fibers (Fig. 1.b) are extracted from it. This plant is known for producing strong, lightweight fibers that are increasingly used in sustainable composite materials.

Notably, Curauá fiber is a natural lignocellulosic material, and it has been utilized in the form of woven mats. The raw fiber was subjected to an alkali treatment, it was done to strengthen the fiber-matrix bond by eliminating surface impurities and increasing surface roughness, ultimately leading to improved adhesion within composite materials. Some physical and mechanical properties of Curauá fiber is presented in Table 1.

Carbon fiber (Fig. 1.c), in the form of a unidirectional mat, was incorporated as a synthetic reinforcement to enhance the mechanical properties of the composites and enable detailed characterization. The carbon fiber used had a tensile strength of 3800 MPa, modulus of elasticity of 230 GPa, fiber diameter of 7 μm, and an areal density of 200 g/m^2.

The combination of these two fibers leverages the sustainable, energy-absorbing characteristics of Curauá fiber with the structural reinforcement of carbon fiber.

An unsaturated polyester resin (Fig. 2) served as the matrix material, selected for its favorable mechanical properties, ease of processing, room-temperature curing capability, and good adhesion to both natural and synthetic fibers. The resin had a viscosity of 450–550 cps at 25°C, density of 1.12 g/cm^3 , gel time of 12–15 min (with 1% MEKP catalyst at 25°C), and a tensile strength of 55 MPa. The curing was carried out at room temperature using methyl ethyl ketone peroxide (MEKP) as the hardener at 1.5 wt% of the resin.

Fig. 3 compares the surface morphology of Curauá fibre before and after alkali treatment. As shown in Fig. 3(a), the untreated fibre exhibits a rough, irregular surface with substantial adhered deposits, flaky material, and surface impurities. These features are consistent with the presence of non-cellulosic constituents and naturally occurring surface residues. In contrast, Fig. 3(b) shows a comparatively cleaner fibre surface with more distinct longitudinal grooves and exposed fibrillar structures following alkali treatment. The reduction in visible surface deposits suggests that the treatment may have removed some surface impurities and non-cellulosic constituents. The resulting surface topography may promote improved polyester resin wetting and mechanical interlocking during composite fabrication.

2.2. Composite fabrication

Fig. 4 represents the flow chart of the Curauá-carbon fiber composites fabrication process. The hybrid composite specimens were fabricated using the hand lay-up technique, followed by compression molding (Fig. 5) to ensure uniform consolidation and proper curing.

Curauá fiber, carbon fiber, and unsaturated polyester resin were combined in distinct weight ratios, as presented in Table 2.

Table 2 outlines the composition of five fabricated composite laminates, all containing a constant 60% of Polyester matrix and varying proportions of Curauá and Carbon fibers. Specimen Cu40-Po60 comprises 40% Curauá fiber with no Carbon fiber, whereas Ca40-Po60 contains 40% Carbon fiber without any Curauá fiber. The remaining three specimens are hybrid composites: Cu20-Ca20-Po60 includes 20% each of Curauá and Carbon fibers; Cu15-Ca25-Po60 consists of 15% Curauá and 25% Carbon fibers; and Cu25-Ca15-Po60 has 25% Curauá



Fig. 1. (a) Extracted raw Curauá fibers, (b) Curauá fiber fabric, and (b) Carbon fiber fabric.

Table 1
Physical and mechanical properties of [39].

Fibers	Density (g/cm^3)	Tensile strength (MPa)	Young's Modulus (GPa)
Curauá fiber	0.57 – 0.92	117 – 3000	27 – 80



Fig. 2. Polyester resin.

and 15% Carbon fibers. This compositional variation facilitates the investigation of how different fiber ratios influence the performance characteristics of the composites. The Cu40-Po60 formulation (40 wt% Curauá fiber and 60 wt% polyester) was selected as the primary reference composition because it represents the non-hybrid natural-fiber composite. This allows the effects of partially replacing Curauá fibers with carbon fibers to be evaluated while maintaining constant total reinforcement (40 wt%) and polyester matrix (60 wt%) contents. The Ca40-Po60 formulation was also included as a carbon-only reference, enabling comparisons between the hybrid composites and both single-fiber systems. Similar comparative approaches have been adopted in previous studies on Curauá/glass [41] and Curauá/basalt [34] hybrid composites. All composites laminate maintained a constant matrix content, while the fiber ratios were varied to evaluate the effect of hybridization on mechanical performance.

A nominal thickness of 3 mm was selected for the specimens to ensure uniformity of the laminates and to have a reliable comparative characterization of Curauá–carbon fiber-reinforced polyester composites. The chosen thickness was found to be optimal for the incorporation

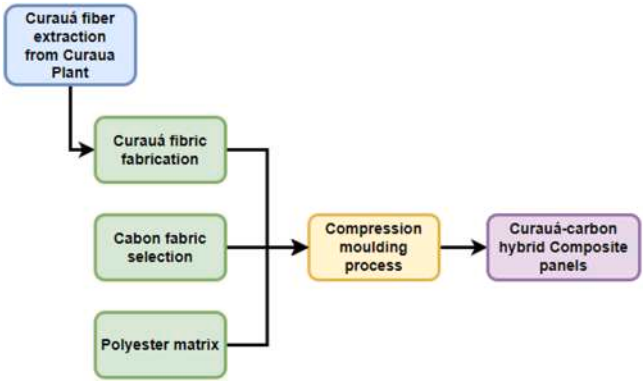

Fig. 4. Curauá-carbon fiber composite fabrication process.

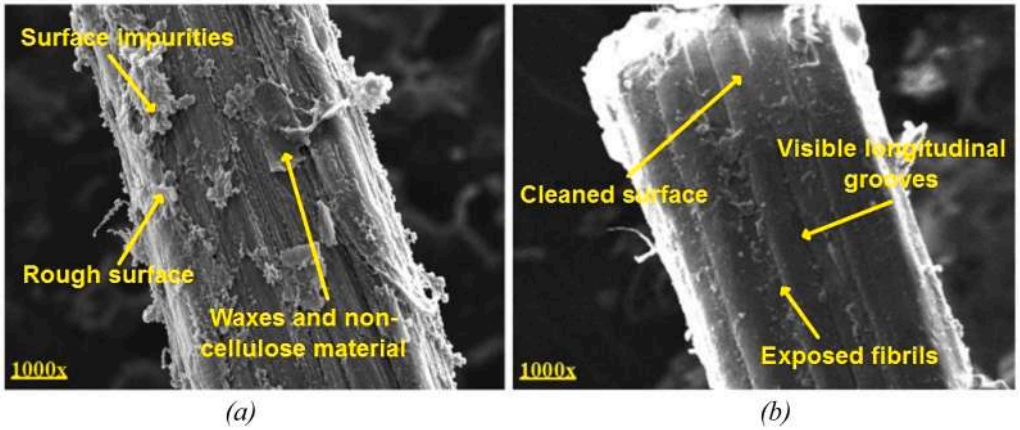

Fig. 3. SEM micrographs of Curauá fibre: (a) before alkali treatment and (b) after alkali treatment.



Fig. 5. Compression moulding machine.

Table 2
Composition of prepared specimens.

Specimen code	Curauá fiber (%)	Carbon fiber (%)	Polyester matrix (%)	To achieve the final thickess (mm)	Number of samples used for each type of test
Cu40-Po60	40	0	60	3	4
Ca40-Po60	0	40	60	3	4
Cu20-Ca20-Po60	20	20	60	3	4
Cu15-Ca25-Po60	15	25	60	3	4
Cu25-Ca15-Po60	25	15	60	3	4

of reinforcing fiber fabrics and the polyester matrix, which allows resin impregnation and consolidation during compression molding. Moreover, maintaining a constant thickness across all composite formulations minimizes geometrical variations and allows the influence of fiber hybridization on mechanical and physical properties to be assessed under comparable conditions.

This selection is consistent with the general testing principles of ASTM D3039/D3039M for tensile characterization, ASTM D790 for flexural characterization, and ASTM D570 [52] for water absorption evaluation, provided the specimen geometry and testing requirements are met. Therefore, 3 mm thickness was chosen as a design criterion for production purposes instead of being an explicitly required dimension according to the standards mentioned above.

Woven mats of Curauá fiber and unidirectional carbon fibers were cut to dimensions of 300 mm × 300 mm (Fig. 6) to match the mold cavity size used during fabrication. For each composite laminate, the fiber layers were stacked according to the designed composition, ensuring uniform distribution and orientation. The polyester resin was mixed thoroughly with methyl ethyl ketone peroxide hardener at the recommended ratio and applied evenly over each fiber layer to achieve complete wetting. The lay-up was then subjected to compression molding at room temperature under a load of approximately 5 MPa for 24 h to ensure proper compaction and resin curing. After demolding, the composite laminates were post-cured in a hot air oven at 80 °C for 2 h to improve crosslinking and thermal stability. Specimens (Fig. 6) were then cut from the laminates as per ASTM standards for subsequent mechanical characterization.



(a) (b)

Fig. 6. Composite sample: (a) Cu40-Po60, and (b) Ca40-Po60.

The composite laminates were fabricated using Curauá fiber mats (Cu), carbon fiber mats (Ca), and polyester resin (Po) as the matrix. Curauá fibers were arranged as woven mats, whereas carbon fibers were arranged as unidirectional mats. Five composite configurations were prepared by varying the fibre weight percentages and stacking sequences while maintaining a nominal laminate thickness of 3 mm. Initially, the fiber mats were cut to the required mould dimensions, and the mould surface was cleaned and coated with a suitable release agent. The polyester resin was prepared according to the recommended resin-to-catalyst ratio and applied uniformly to the reinforcement layers to ensure adequate impregnation. The impregnated layers were then stacked sequentially according to the prescribed configurations, as illustrated in Fig. 7. The Cu40–Po60 laminate consisted of three Curauá layers arranged in a Cu/Cu/Cu sequence, whereas the Ca40–Po60 laminate comprised three carbon layers arranged in a Ca/Ca/Ca sequence. For the Cu20–Ca20–Po60 hybrid laminate, two Curauá layers were placed on either side of a carbon layer (Cu/Ca/Cu). The Cu15–Ca25–Po60 configuration consisted of one Curauá layer followed by two carbon layers (Cu/Ca/Ca), while the Cu25–Ca15–Po60 configuration comprised two Curauá layers followed by one carbon layer (Cu/Cu/Ca). In all configurations, the polyester resin was used to impregnate the reinforcement and bind the layers together. The overall reinforcement content was maintained at 40 wt% and the polyester resin content at 60 wt%, with the relative proportions of Curauá and carbon fibres varied according to the designated formulation. After stacking, the mould assembly was consolidated using the prescribed fabrication procedure to minimise void formation and maintain the required laminate thickness. The laminates were subsequently cured under the specified processing conditions and removed from the mould after curing. The consolidated panels were then cut into specimens of the dimensions required for mechanical testing, and their dimensions were checked before testing. The nominal thickness of each laminate was maintained at 3 mm.

2.3. Physical, mechanical and thermal characterizations

The physical and thermo-mechanical performances of the composite specimens were evaluated through a series of physical, mechanical, and thermal tests.

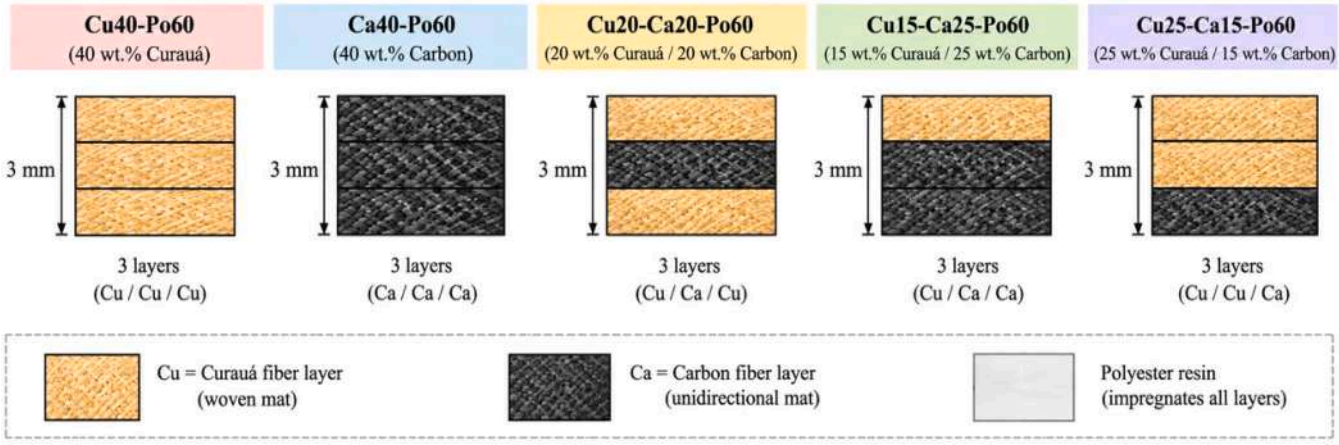

Fig. 7. Fabrication procedure: stacking configuration for each fiber composition/sample.

2.3.1. Determination Physical Properties

2.3.1.1. Water absorption. The water absorption (WA) behavior of the composites was evaluated using a gravimetric immersion procedure based on ASTM D570 [52]. The specimens were prepared from compression-molded composite laminates with a nominal thickness of 3 mm. Moreover, the aforementioned thickness was maintained to ensure consistency with respect to the fabricated laminates, and to analyze the absorption of moisture on the same basis as the composite was characterized. ASTM D570 permits testing of sheet materials at their actual thickness, although specific specimen dimensions and conditioning requirements must be considered when claiming full standard compliance.

The composite specimens (Fig. 8a) were immersed in distilled water (pH 7) for durations of 8, 16, and 24 h (Fig. 8b), and their weights were measured at specified intervals. Before immersion, the specimens were air-dried under the sun for 24 h, and then their mass was recorded. After the specified time, the specimens were taken out, the excess moisture was wiped off using a cotton cloth, and then the wet mass was recorded with the help of a weighing balance. The percentage water absorption of the material was determined using Eq. (1). The methodology was adapted to study the short-term moisture uptake property of the Curauá-carbon/polyester composites. The percentage of water absorption was calculated using the standard formula [53].

$$WA(\%) = \frac{(W_t - W_0)}{W_0} X \quad 100 \tag{1}$$

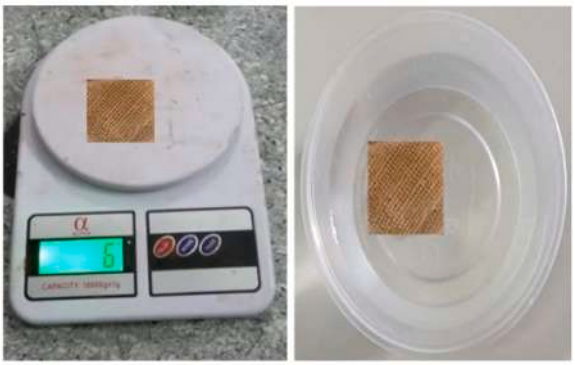

(a) (b)

Fig. 8. (a) Specimen before immersion, and (b) Specimen immersed in water.

where, W_t denotes the weight of the sample after immersion, while W_0 refers to the dry weight of the sample in its dry state before immersion.

2.3.1.2. Scanning electron microscopy (SEM) Analysis. Additionally, scanning electron microscopy (SEM) analysis was conducted to closely examine the fracture surfaces and the fiber–matrix interface morphology of the composites. SEM provided high-resolution images that revealed critical details such as fiber pull-out, matrix cracking, voids, and fiber breakage. These features helped in understanding the underlying failure mechanisms, such as poor adhesion at the interface or stress concentration zones that led to crack initiation and propagation. The quality of interfacial bonding between the Curauá and carbon fibers with the polyester matrix was also assessed, as it plays a crucial role in effective load transfer and overall mechanical performance.

2.3.2. Determination of mechanical properties

Fig. 9 represents various sample sizes used for hardness, tensile, flexural, and impact tests.

The specimens were prepared according to ASTM standards [54] with the following dimensions: Hardness – 100 mm × 10 mm × 3 mm (as per ASTM D785), Tensile – 250 mm × 25 mm × 3 mm (ASTM

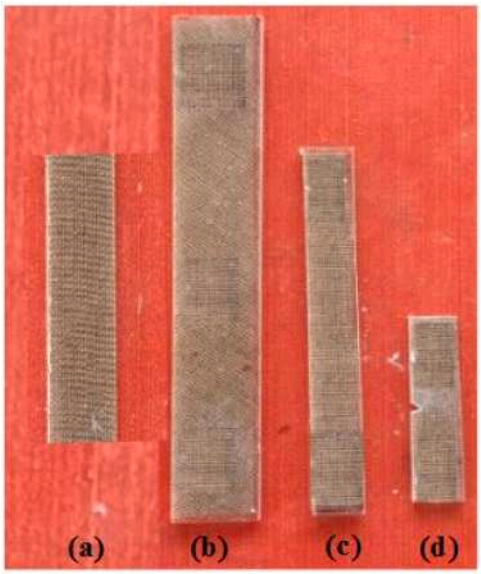

Fig. 9. Samples used for mechanical tests: (a) hardness test (100 mm × 10 mm × 3 mm), (b) tensile strength test (250 mm × 25 mm × 3 mm), (c) flexural test (127 mm × 12.7 mm × 3 mm), (d) impact test (63.5 mm × 12.7 mm × 3 mm).

D3039), Flexural – 127 mm × 12.7 mm × 3 mm (as per ASTM D790), and Impact – 63.5 mm × 12.7 mm × 3 mm with a V-notch depth of 2.54 mm and notch tip radius of 0.25 mm (as per ASTM D256). Fig. 10 (a) illustrates the Universal Testing Machine (UTM), which was used to perform tests. The UTM used in this study is a computerized, servo-controlled model with a maximum load capacity of 100 kN. It features a high-precision load cell, an extensometer for accurate strain measurements, and adjustable crosshead speeds ranging from 0.5 to 500 mm/min. This setup ensures consistent and reliable testing conditions. Fig. 10(b) shows a close-up view of the specimen being tested in the UTM.

Hardness was measured using a Rockwell hardness tester to determine the surface resistance of the composites to indentation in accordance with ASTM D785. The tests were performed using a manually operated Rockwell-type hardness testing machine (Make: Fine Testing Instruments Pvt. Ltd. (FIE), Model: RASRB) as shown in Fig. 11, equipped with a 1/16-inch diameter steel ball indenter, applying a minor load of 10 kgf followed by a major load of 100 kgf corresponding to the Rockwell B scale (HRB). The Rockwell B scale is suitable for rigid polymer composites and fiber-reinforced thermoset materials where sufficient stiffness permits reliable indentation measurement. The hardness values were recorded after an appropriate dwell time to ensure measurement consistency and repeatability. Tensile testing was performed according to ASTM D3039 [55] to obtain ultimate tensile strength, young's modulus, and elongation at break.

Flexural properties, including bending strength and flexural modulus, were assessed using ASTM D790 [56]. Interlaminar shear strength was evaluated via ASTM D5379 [57] to understand fiber-matrix bonding quality. Impact resistance was determined using the Izod impact test following ASTM D256 [58], which measures energy absorption under sudden loading. Fig. 12 illustrates the flexural test before Fig. 12 (a) and after Fig. 12 (b).

2.3.3. Determination thermal properties

Thermal stability and degradation behavior were examined by thermogravimetric analysis (TGA), conducted in accordance with ASTM E1131–20 [59] using a PerkinElmer TGA 4000 system. The samples were heated from room temperature up to 800 °C at a constant heating rate of 10 °C/min under a nitrogen atmosphere with a flow rate of 20 mL/min. The instrument continuously monitored the weight loss to determine the thermal degradation profile and stability of the composites.

2.3.4. Statistical Analysis

One-way analysis of variance (ANOVA) was performed using Minitab statistical software to evaluate the effect of composite configuration on the mechanical properties of the fabricated laminates. Five composite configurations, namely Cu40–Po60, Ca40–Po60, Cu20–Ca20–Po60, Cu15–Ca25–Po60, and Cu25–Ca15–Po60, were considered for statistical comparison. Separate ANOVA analyses were conducted for hardness, tensile strength, tensile modulus, flexural strength, flexural modulus, shear strength, and impact strength, using four replicate specimens for each configuration. The statistical significance of differences among the group means was evaluated using the F-statistic and corresponding P-value, with a significance level of 0.05. A P-value below 0.05 was considered to indicate a statistically significant difference among the composite configurations. The ANOVA results were expressed in terms of degrees of freedom (DF), adjusted sum of squares (Adj SS), adjusted mean squares (Adj MS), F-values, and P-values.



(a) (b)

Fig. 10. (a) universal testing machine used and (b) sample closed view during the tensile strength test.



Fig. 11. Hardness testing device.

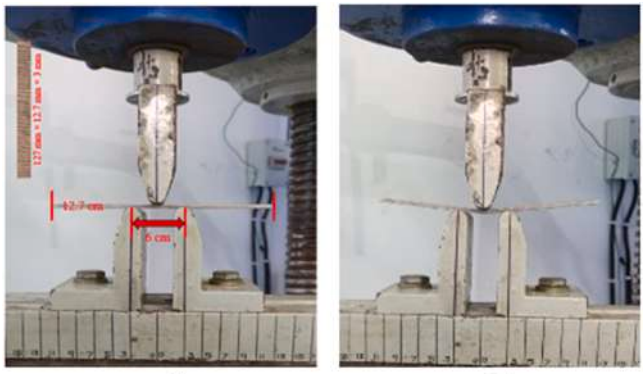

(a) (b)

Fig. 12. Flexural test: (a) before and (b) during the test.

3. Results and discussion

During this experimental campaign, the physical, mechanical, and thermal performances of the hybridized composite fiber, fabricated with natural (Curauá) and man-made (carbon) fibers, are evaluated. The results highlight the synergistic interaction between natural and synthetic fibers, which led to improved interfacial bonding and energy dissipation. The findings suggest that such hybrid composites are well-suited

for demanding engineering applications requiring both mechanical robustness and environmental resilience.

3.1. Physical properties

3.1.1. Water absorption test

The water absorption behavior of the composite specimens, evaluated after 8, 16, and 24 h of immersion in distilled water, reveals distinct trends based on fiber composition as presented in Fig. 13.

Specimen Cu40–Po60, containing 40% curauá fiber and no carbon fiber, exhibited the highest water uptake, reaching 8.2% after 24 h. This behavior is attributed to the hydrophilic nature of natural curauá fibers, which readily absorb moisture due to their cellulose content. In contrast, specimen Ca40–Po60, composed entirely of 40% carbon fiber and 60% polyester, showed the lowest water absorption of 1.6% after 24 h, since carbon fibers are inherently hydrophobic and resist moisture ingress. The hybrid composites (Cu20–Ca20–Po60, Cu15–Ca25–Po60, and Cu25–Ca15–Po60) demonstrated intermediate water absorption values. Among them, Cu25–Ca15–Po60 exhibited comparatively lower water uptake of 2.7% after 24 h, whereas, for Cu20–Ca20–Po60, Cu15–Ca25–Po60 these values are 4.2% and 3.1%, rspectively. Although curauá fibers are hydrophilic in nature, the reduced moisture absorption observed in this hybrid configuration can be attributed to the presence of hydrophobic carbon fibers, which act as a barrier to moisture diffusion and reduce capillary transport within the composite structure. In addition, improved fiber packing and reduced microvoid formation in the hybrid laminate may have further restricted water penetration. It is also observed that the water absorption tends to approach saturation at 24 h, beyond which no significant increase in weight gain was recorded. This indicates that the composite specimens had reached their equilibrium moisture content within the studied duration.

These results align with findings by [60] who reported that natural fibers increase moisture absorption due to their cellulose content, whereas carbon fibers reduce water uptake because of their hydrophobic nature. The hybridization of natural and carbon fibers, as in specimen S5, combines the advantages of both materials, enhancing water resistance and composite durability.

3.1.2. Morphological analysis

The scanning electron microscopy (SEM) analysis was conducted on the fractured surfaces of specimens S1 (Fig. 14.a) and S5 (Fig. 14.b) to investigate the microstructural features influencing their tensile behavior as illustrated in Fig. 15. The SEM analysis has been performed after the tensile strength tests (please see Section 3.2.2), and the best (S5) and worst (S1) specimens have been selected for the SEM analysis.

For the specimen Cu40-Po60 (composed of 40% Curauá fiber and 60% polyester matrix), the SEM image revealed a rough and irregular fracture surface with evident fiber pull-out, micro-cracks, and poor interfacial bonding between the Curauá fibers and the polyester matrix. These morphological features indicate inadequate stress transfer and weak adhesion, which contributed to the lower tensile performance. In contrast, the specimen Cu25-Ca15-Po60 (containing 25% Curauá fiber, 15% carbon fiber, and 60% polyester) demonstrated a significantly higher tensile strength (see Section 3.2.2). The SEM image of Cu25-Ca15-Po60 reveals a denser and more uniform microstructure, with well-embedded carbon fibers and fewer signs of fiber debonding or voids. The improved fiber–matrix adhesion and the reinforcing effect of carbon fibers led to better load distribution and reduced crack propagation. Overall, the SEM observations align with the tensile test results, confirming that the addition of carbon fiber in Cu25-Ca15-Po60 enhanced the structural integrity and mechanical performance of the composite.

3.2. Mechanical properties

The mechanical properties of reference and hybrid composite samples comprising of various proportions of Curauá fiber fabric (Cu), carbon fiber fabric (Ca), and a polymer matrix (Po) are presented in Table 3. The results show that the inclusion of Curauá fiber fabric contributes meaningfully to the mechanical behavior of the composites. The Cu25–Ca15–Po60 specimens, which contain the highest Curauá fiber proportion, have demonstrated the highest hardness (84.75), flexural strength (125.5 MPa), and tensile modulus (5.8 GPa), indicating a significant reinforcing effect from the Curauá fiber. Furthermore, the presence of Curauá in hybrid compositions enhanced the overall ductility and impact resistance of the composites. Beyond mechanical contributions, Curauá fiber fabric adds significant value in terms of sustainability, cost-efficiency, and reduced environmental footprint.

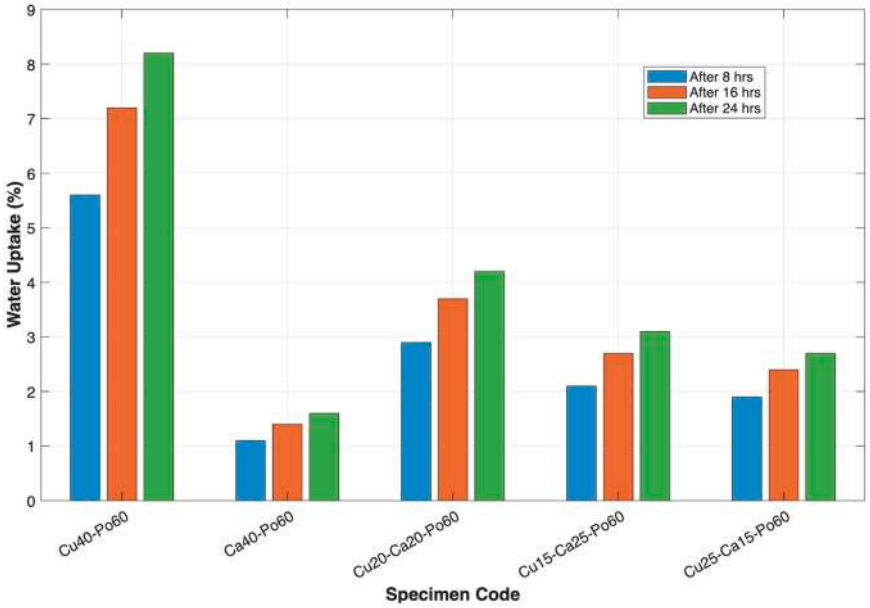

Fig. 13. Water uptake percentage.

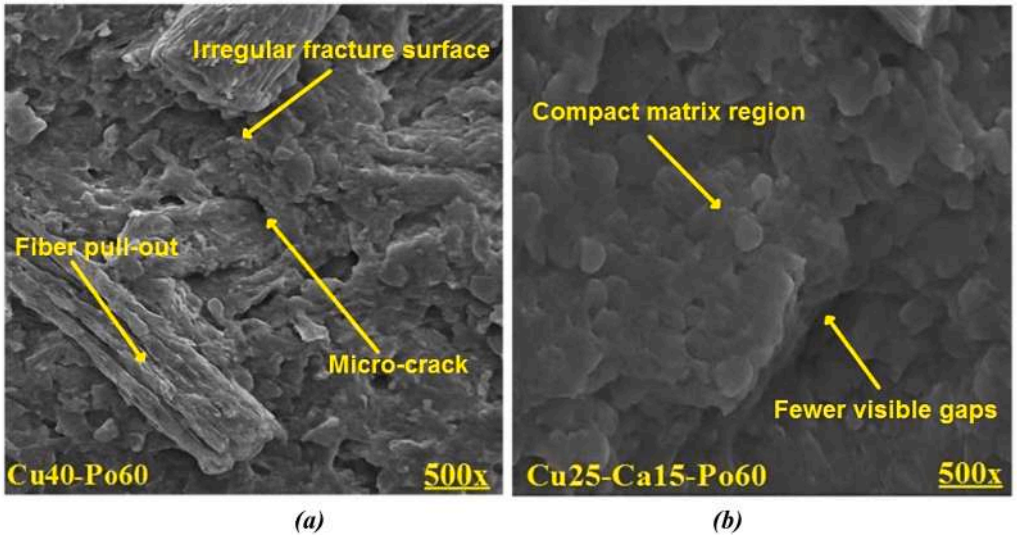

Fig. 14. SEM analysis: (a) Cu40-Po60, and (b) Cu25-Ca15-Po60.

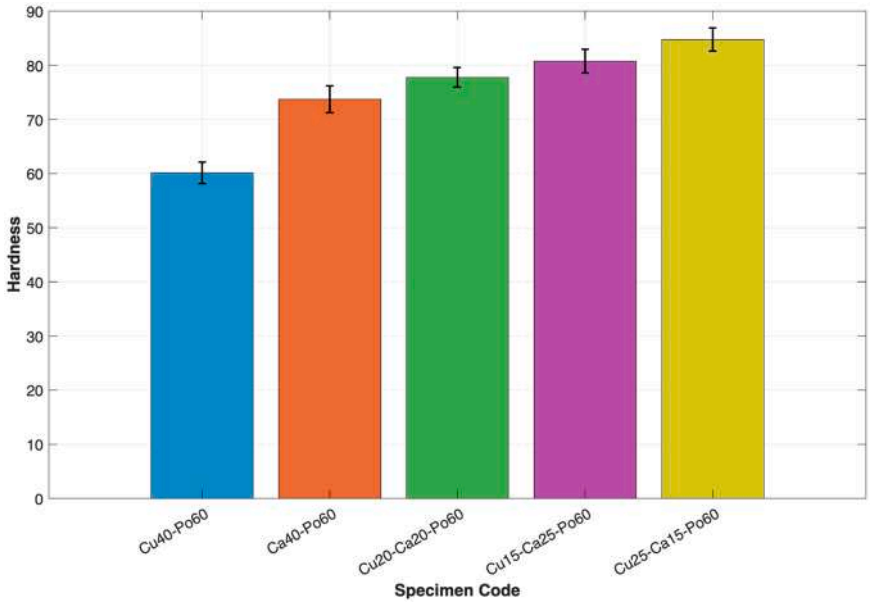

Fig. 15. Hardness of the tested samples.

Table 3
Mechanical properties of reference and hybrid composite formulations (mean ± SD).

Specimen code	Hardness (HRB)	Tensile strength (MPa)	Tensile modulus (GPa)	Flexural strength (MPa)	Flexural modulus (GPa)	Shear strength (MPa)	Impact strength (J/m)
Cu40-Po60	60.14 ± 1.00	52.25 ± 0.83	2.80 ± 0.07	75.25 ± 0.83	2.50 ± 0.07	14.03 ± 0.19	18.10 ± 0.22
Ca40-Po60	73.75 ± 0.83	104.75 ± 0.83	6.50 ± 0.07	120.75 ± 1.49	5.80 ± 0.07	30.00 ± 0.19	10.03 ± 0.15
Cu20-Ca20-Po60	77.75 ± 0.83	88.00 ± 0.70	4.80 ± 0.07	105.00 ± 0.70	4.50 ± 0.07	23.98 ± 0.19	15.05 ± 0.11
Cu15-Ca25-Po60	80.75 ± 0.83	94.75 ± 0.83	5.20 ± 0.07	112.50 ± 1.11	5.20 ± 0.07	27.05 ± 0.11	16.03 ± 0.15
Cu25-Ca15-Po60	84.75 ± 0.83	109.75 ± 0.83	5.80 ± 0.07	125.50 ± 1.12	5.50 ± 0.07	32.08 ± 0.23	20.08 ± 0.19

where, SD is the standard deviation

The results also showed good consistency, with coefficients of variation generally below 6%, confirming the reliability of the experimental process. Overall, the inclusion of Curauá fiber enhances the multifunctional performance of composite samples while supporting the development of greener material solutions.

3.2.1. Hardness evaluation

The hardness results of the specimens indicate a clear increasing trend from Cu40-Po60 to Cu25-Ca15-Po60 as illustrated in Fig. 15.

The hardness values of the composite specimens exhibited a consistent increasing trend with the incorporation of carbon fiber, either individually or in hybrid combinations with Curauá fiber. Using the specimen Cu40-Po60, reinforced solely with 40% Curauá fiber and recording a hardness of 60.138 HR, the addition of carbon fiber led to notable improvements. Ca40-Po60, which contains 40% carbon fiber, showed a 22.64% increase in hardness. Hybrid composites further enhanced this property: Cu20-Ca20-Po60, Cu15-Ca25-Po60, and Cu25-Ca15-Po60 exhibited increases of 29.27%, 34.27%, and 40.88%, respectively. This progressive improvement demonstrates the significant role of carbon fiber in enhancing surface resistance while also highlighting the effectiveness of hybrid fiber systems in optimizing hardness performance through synergistic reinforcement [61].

Although carbon fiber generally contributes more significantly to stiffness and hardness than natural fibers, the superior hardness observed in the Cu25-Ca15-Po60 specimen compared with Cu15-Ca25-Po60 can be attributed to the optimized hybridization effect between curauá fiber, carbon fiber, and the polyester matrix. The slightly higher curauá fiber fraction may have improved fiber dispersion and stress distribution within the matrix due to its relatively rough surface morphology, which enhances mechanical interlocking and fiber–matrix adhesion [62]. In contrast, higher carbon fiber content can sometimes lead to localized fiber clustering and reduced matrix wetting because of its relatively smooth surface characteristics. Therefore, the balanced hybrid composition in Cu25-Ca15-Po60 likely promoted more efficient stress transfer, reduced microvoid formation, and improved resistance to localized plastic deformation during indentation, resulting in enhanced hardness performance [63].

This trend suggests a synergistic effect between the natural and synthetic fibers, where the combination optimizes the composite's resistance to surface deformation. The enhanced hardness in these hybrids can be attributed to the improved fiber–matrix interaction and the reinforcing effect of carbon fiber, even at moderate content levels [64]. Overall, the results imply that incorporating a balanced hybrid fiber system leverages the sustainability benefits of natural fibers while significantly improving the mechanical surface properties.

3.2.2. Tensile strength and tensile modulus properties

The tensile strength and tensile modulus results of the composite specimens show a distinct enhancement based on the type and proportion of fiber reinforcement used, as illustrated in Fig. 16.

The tensile strength analysis reveals a consistent improvement across the composite specimens with the incorporation of carbon fiber, either fully or in hybrid form. Taking Cu40-Po60 (reinforced solely with Curauá fiber) as the baseline, all other configurations demonstrated significant percentage increases [65]. Specimen Ca40-Po60, reinforced entirely with carbon fiber, exhibited a 100.38% increase in tensile strength compared to Cu40-Po60, highlighting the superior reinforcing ability of synthetic fibers [66]. The hybrid specimens also showed notable improvements: Cu20-Ca20-Po60 increased by 68.41%, Cu15-Ca25-Po60 by 81.25%, and Cu25-Ca15-Po60 recorded the highest increase of 109.98%. These findings confirm that both the type and proportion of fiber reinforcement significantly influence tensile performance. The superior tensile strength observed in Cu25-Ca15-Po60 compared with Cu15-Ca25-Po60 suggests that an optimized hybrid composition improved fiber dispersion and interfacial bonding between the fibers and polyester matrix, enabling more efficient stress transfer and delaying crack initiation during tensile loading. The relatively rough surface morphology of curauá fiber may also have enhanced mechanical interlocking with the matrix, compensating for the slightly lower carbon fiber content and resulting in improved load-sharing efficiency within the hybrid structure [67].

The tensile modulus results further support the tensile strength observations by demonstrating the influence of reinforcement composition on the stiffness of the composites. The specimen Cu40-Po60 exhibited the lowest stiffness among the tested samples and is therefore considered the baseline for comparison. In contrast, the Ca40-Po60 specimen, reinforced with 40% carbon fiber, showed the highest stiffness, indicating an improvement of 132.14% over the baseline. Among the hybrid composites, Cu25-Ca15-Po60 showed a 107.14% increase in tensile modulus, followed by Cu15-Ca25-Po60 and Cu20-Ca20-Po60 with improvements of 85.71% and 71.43%, respectively. These results clearly demonstrate that incorporating carbon fiber, either individually or in combination with curauá fiber, significantly enhances the stiffness of the composite due to its inherently higher modulus and superior load-

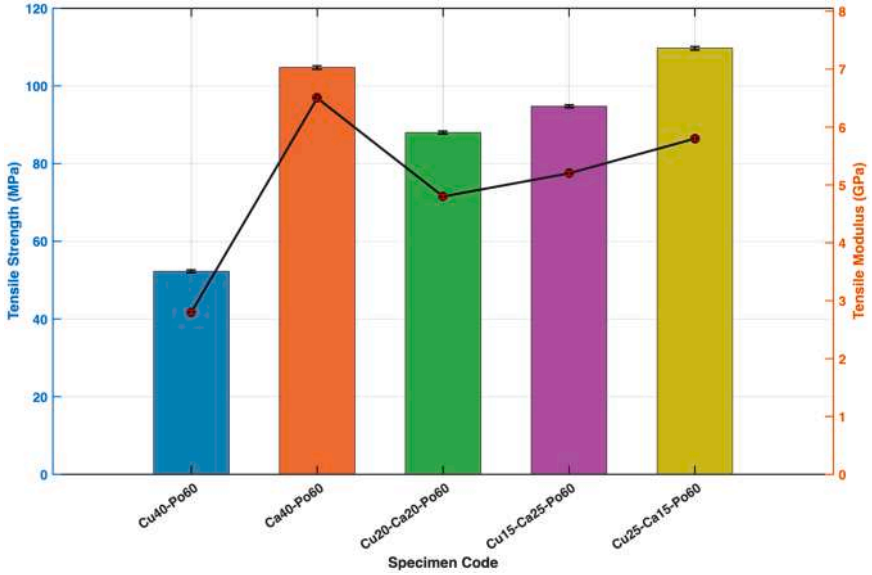

Fig. 16. Tensile strengths and tensile modulus of the tested samples.

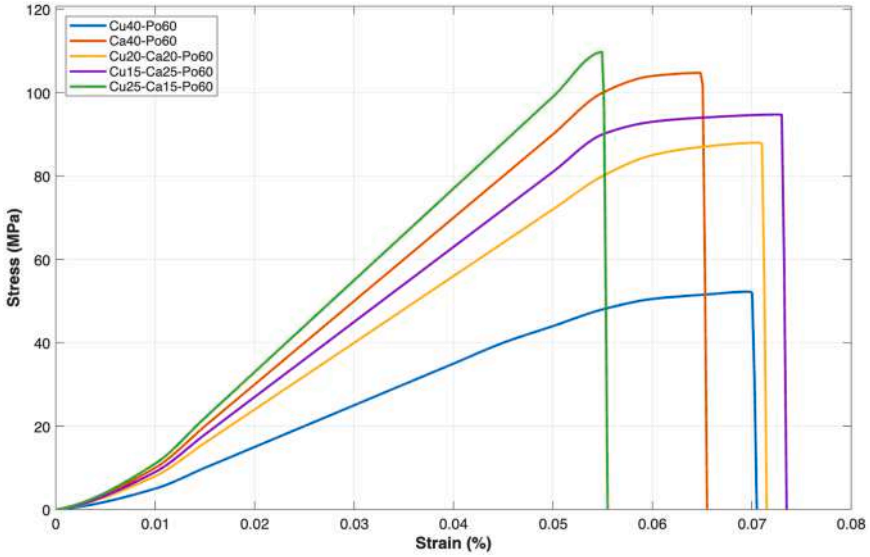

Fig. 17. Stress Vs. strain curves of the tested samples.

bearing capability within the polyester matrix [68]. Furthermore, the relatively higher modulus observed in the Cu25-Ca15-Po60 hybrid specimen compared with other hybrid combinations indicates that the balanced reinforcement ratio contributed to improved stress distribution and reduced microvoid formation, thereby enhancing the overall structural integrity of the composite [69].

The stress–strain behavior of the composite specimens S1 through S5, as illustrated in Fig. 17, highlights the influence of fiber composition on tensile performance.

The tensile behavior of the composite specimens was analyzed based on the stress–strain response under uniaxial loading. All specimens exhibited an initial linear increase in stress with strain, indicating elastic deformation, followed by a peak stress point and a subsequent sharp drop, signifying failure. Among the tested composites, the Cu40-Po60 specimen, reinforced with 40% curaua fiber, showed the lowest tensile strength and stiffness, though it sustained a relatively higher strain before failure, indicating ductile characteristics. In contrast, the Ca40-Po60 specimen, reinforced with 40% carbon fiber, displayed the steepest slope in the initial region of the curve, reflecting high stiffness, and attained a peak tensile strength of 104.75 MPa at a strain of 0.65%, followed by a sudden failure typical of brittle behavior. The hybrid composites demonstrated improved performance, combining the ductility of curaua with the stiffness of carbon fiber. Specifically, Cu20-Ca20-Po60 and Cu15-Ca25-Po60 exhibited balanced mechanical responses, with the latter achieving a peak strength of 94.75 MPa at 0.7% strain. Notably, Cu25-Ca15-Po60 recorded the highest tensile strength of 109.75 MPa at 0.055% strain but failed abruptly, indicating a trade-off between strength and ductility. Overall, the incorporation of carbon fiber significantly enhanced tensile properties, while the hybridization strategy offered an effective means of tailoring the composite behavior by optimizing strength, stiffness, and failure strain [70].

3.2.3. *Flexural strength and flexural modulus properties*

The flexural strength and flexural modulus results of the developed composites demonstrate a strong dependence on the type and proportion of fiber reinforcement, as illustrated in Fig. 18.

The specimen Cu40-Po60 is considered the baseline for comparison, as it exhibited the lowest flexural strength (75.25 MPa) and flexural

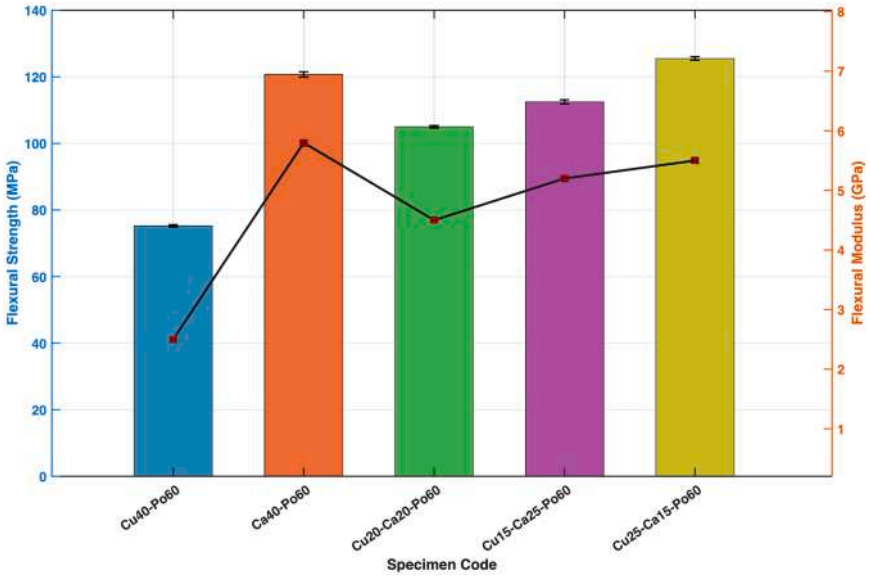

Fig. 18. Flexural strength and flexural modulus of all tested samples.

modulus (2.5 GPa). The specimen Ca40-Po60, reinforced solely with carbon fiber, showed a significant improvement in flexural strength and modulus by 60.46% and 132.00%, respectively, compared with the baseline specimen. This substantial increase confirms the superior stiffness and load-bearing capability of carbon fiber within the polyester matrix under bending conditions [71]. Among the hybrid composites, the specimen Cu20-Ca20-Po60 exhibited improvements of 39.53% in flexural strength and 80.00% in flexural modulus compared with Cu40-Po60, demonstrating the effectiveness of balanced hybrid reinforcement in enhancing bending performance. Similarly, Cu15-Ca25-Po60 showed further improvements of 49.50% in flexural strength and 108.00% in flexural modulus, indicating that increasing carbon fiber content generally enhances resistance to bending deformation due to improved stiffness contribution [72].

Interestingly, the specimen Cu25-Ca15-Po60 exhibited the highest flexural strength among all tested composites, showing an improvement of 66.78% compared with Cu40-Po60, while also achieving a significant increase of 120.00% in flexural modulus. Notably, the flexural strength of Cu25-Ca15-Po60 exceeded that of the fully carbon fiber–reinforced specimen Ca40-Po60 by approximately 3.93%, highlighting the effectiveness of hybridization in optimizing bending performance. This superior behavior can be attributed to the synergistic interaction between curauá and carbon fibers, where the relatively rough surface morphology of curauá fibers enhances mechanical interlocking with the polyester matrix and improves stress distribution during bending [44]. At the same time, carbon fibers contribute high stiffness and load-bearing capacity, resulting in improved resistance to tensile and compressive stresses generated on opposite sides of the specimen under flexural loading [73]. Furthermore, the optimized hybrid composition in Cu25-Ca15-Po60 likely promoted improved fiber dispersion and reduced microvoid formation compared with composites containing higher carbon fiber content, where fiber clustering and limited matrix wetting may occur. This improved interfacial bonding enhances stress transfer efficiency and delays crack initiation and propagation during bending, thereby resulting in superior flexural strength and modulus. Overall, the results demonstrate that an optimized hybrid reinforcement strategy can produce composites with improved bending performance compared with single-fiber-reinforced systems.

3.2.4. *Impact resistance*

The impact resistance values illustrated in Fig. 19 highlight the influence of fiber composition on the toughness of the composite specimens.

Specimen Cu40-Po60, containing 40% Curauá fiber, exhibited the highest impact resistance among the single-fiber composites, reflecting the superior energy-absorbing capability of natural fibers due to their relatively higher elongation at break and fibrillar structure, which promotes crack bridging and fiber pull-out during sudden loading conditions. In contrast, Ca40-Po60, reinforced with 40% carbon fiber, showed the lowest impact resistance, indicating that although carbon fibers significantly improve stiffness and strength, their brittle nature reduces the ability of the composite to dissipate impact energy effectively [74]. The hybrid specimens (Cu20-Ca20-Po60, Cu15-Ca25-Po60, and Cu25-Ca15-Po60) demonstrated notable improvements in impact resistance compared with Ca40-Po60, with increases of approximately 50.1%, 59.8%, and 100.2%, respectively. These improvements clearly indicate that hybridization enhances the toughness of the composites by combining the energy-absorbing characteristics of curauá fibers with the structural reinforcement provided by carbon fibers [75].

Among the hybrid configurations, Cu25-Ca15-Po60 exhibited the highest impact resistance, showing an improvement of approximately 10.9% compared with the curauá-only composite (Cu40-Po60). This superior impact performance suggests the presence of an optimized hybrid reinforcement effect in which the slightly higher proportion of curauá fiber enhanced crack propagation resistance through mechanisms such as fiber pull-out, interfacial debonding, and crack deflection during impact loading [76]. At the same time, the incorporation of carbon fiber contributed to improved load-bearing capability and structural stability, preventing catastrophic failure of the composite [77]. Furthermore, the balanced reinforcement ratio in Cu25-Ca15-Po60 likely promoted improved fiber dispersion and stronger interfacial bonding within the polyester matrix, which enhanced stress transfer efficiency and delayed crack initiation under dynamic loading conditions. The synergistic interaction between natural and synthetic fibers therefore resulted in improved energy absorption capability without compromising structural integrity [78]. Overall, the results demonstrate that fiber hybridization can be effectively utilized to enhance the toughness of polyester-based composites while maintaining balanced mechanical performance across multiple loading conditions.

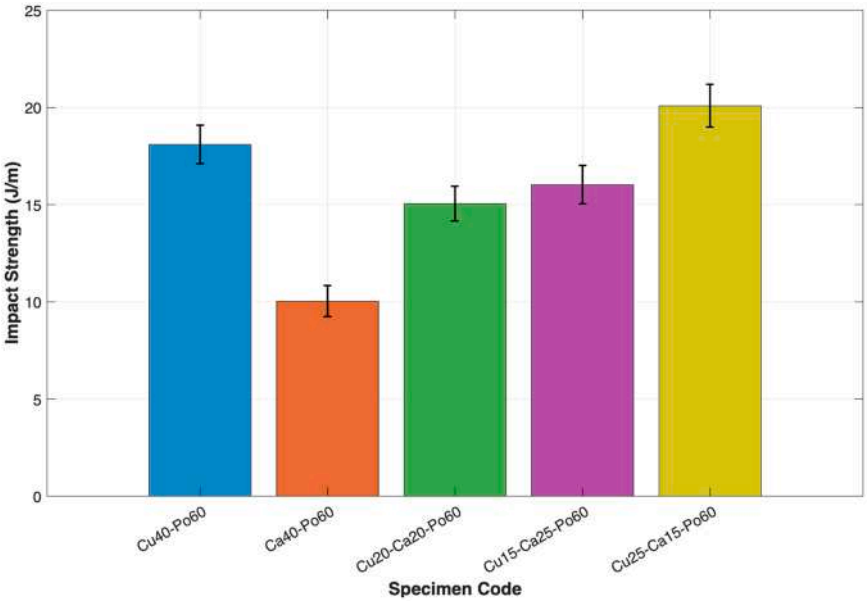

Fig. 19. Impact resistance of all tested samples.

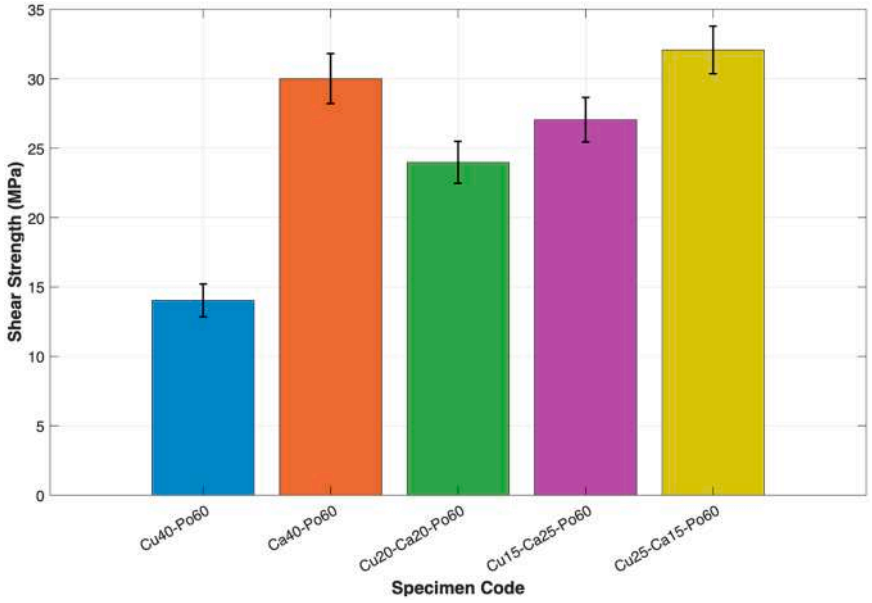

Fig. 20. Shear strength of all tested samples.

3.2.5. *Shear strength*

The shear strength values shown in Fig. 20 illustrate the effect of fiber composition on the composite specimens' resistance to shear forces.

The specimen Cu40-Po60, reinforced solely with 40% curauá fiber, exhibited the lowest shear strength (14.025 MPa) and is therefore considered the baseline for comparison. In contrast, the specimen Ca40-Po60, containing 40% carbon fiber, showed a significant improvement of approximately 113.90% in shear strength compared with the baseline specimen, confirming the superior load-bearing capability and interfacial stress transfer efficiency of carbon fiber within the polyester matrix [79]. Among the hybrid composites, Cu20-Ca20-Po60 exhibited a shear strength of 23.975 MPa, corresponding to an improvement of approximately 70.93% compared with Cu40-Po60. Similarly, the specimen Cu15-Ca25-Po60 showed a further increase in shear strength to 27.05 MPa, representing an improvement of approximately 92.87%, indicating that increasing carbon fiber content generally enhances resistance to interlaminar shear stresses [80].

Interestingly, the specimen Cu25-Ca15-Po60 demonstrated the highest shear strength among all tested configurations, recording a value of 32.075 MPa, which corresponds to an improvement of approximately 128.71% compared with Cu40-Po60 and about 6.92% higher than the carbon fiber–only specimen Ca40-Po60. This superior performance suggests the presence of an optimized hybrid reinforcement effect in which the slightly higher proportion of curauá fiber contributed to improved interfacial bonding through enhanced mechanical interlocking with the polyester matrix [81]. At the same time, the presence of carbon fiber provided the necessary stiffness and resistance to shear deformation, resulting in efficient stress transfer across the fiber–matrix interface [82]. Furthermore, the balanced hybrid composition in Cu25-Ca15-Po60 likely promoted improved fiber dispersion and reduced microvoid formation compared with composites containing higher carbon fiber content, where localized fiber clustering and limited matrix wetting may occur. This improved interfacial integrity enhances resistance to interfacial debonding and shear crack propagation under loading conditions. Overall, the results demonstrate that an optimized

Table 4
Statistical analysis of mechanical properties.

Properties	Source	DF	Adj SS	Adj MS	F-Value	p-Value
Hardness	Specimen Code	4	1428.92	357.230	356.59	**< 0.001**
	Error	15	15.03	1.002	-	-
	Total	19	1443.95	-	-	-
Tensile strength	Specimen Code	4	8236.80	2059.20	2376.00	**< 0.001**
	Error	15	13.00	0.87	-	-
	Total	19	8249.80	-	-	-
Tensile modulus	Specimen Code	4	31.2320	7.80800	1171.20	**< 0.001**
	Error	15	0.1000	0.00667	-	-
	Total	19	31.3320	-	-	-
Flexural strength	Specimen Code	4	6281.70	1570.43	1002.40	**< 0.001**
	Error	15	23.50	1.57	-	-
	Total	19	6305.20	-	-	-
Flexural modulus	Specimen Code	4	27.9200	6.98000	1047.00	**< 0.001**
	Error	15	0.1000	0.00667	-	-
	Total	19	28.0200	-	-	-
Shear strength	Specimen Code	4	799.425	199.856	4329.02	**< 0.001**
	Error	15	0.693	0.046	-	-
	Total	19	800.118	-	-	-
Impact strength	Specimen Code	4	230.057	57.5143	1506.92	**< 0.001**
	Error	15	0.572	0.0382	-	-
	Total	19	230.630	-	-	-

hybrid reinforcement strategy significantly improves the shear performance of polyester-based composites through synergistic interaction between natural and synthetic fibers.

3.2.6. Statistical analysis of mechanical properties

The one-way analysis of variance (ANOVA) results presented in Table 4 demonstrate that composite configuration has a statistically significant effect on all seven mechanical properties, including hardness, tensile strength, tensile modulus, flexural strength, flexural modulus, shear strength, and impact strength. All properties exhibit P-values below 0.001, confirming statistically significant differences among the mean values of the five composite configurations. Among the evaluated properties, shear strength exhibits the highest F-value (4329.02), followed by tensile strength (2376.00), impact strength (1506.92), tensile modulus (1171.20), flexural modulus (1047.00), flexural strength (1002.40), and hardness (356.59). These results indicate that the variations between composite configurations are substantially greater than the variations within each configuration. The high F-values and relatively small error sums of squares suggest that the differences in fiber weight percentage and stacking sequence are associated with pronounced variations in the measured mechanical properties. Overall, the ANOVA results confirm that composite configuration significantly influences the mechanical performance of the developed composites.

3.3. Thermal properties

3.3.1. Thermogravimetric analysis

The thermogravimetric analysis (TGA) data presented in Fig. 21 show that all composite specimens retained 100% of their mass up to 75 °C, with thermal degradation gradually initiating beyond this temperature. Specimen Cu40-Po60, composed entirely of Curauá fiber reinforcement, exhibited the highest weight loss and retained only 12.5% residual mass at 800 °C, indicating comparatively lower thermal stability. In contrast, specimen Cu25-Ca15-Po60, a hybrid composite containing both Curauá and carbon fibers, retained approximately 30% residual mass at 800 °C, demonstrating significantly improved thermal resistance. Similarly, the carbon fiber–rich composite Ca40-Po60 and other hybrid compositions such as Cu20-Ca20-Po60 and Cu15-Ca25-Po60 also exhibited higher residual mass compared to the Curauá-only composite, confirming enhanced thermal stability. The observed thermal degradation trend is consistent with the TGA behavior of hybrid fiber-reinforced composites, where the incorporation of thermally stable carbon fibers improves resistance to high-temperature decomposition. The higher residual mass observed in carbon fiber-containing specimens is mainly attributed to the superior thermal stability and inert characteristics of carbon fibers, which delay degradation and improve char formation at elevated temperatures [83].

4. Integrated Performance Index (IPI) and ranking of composite formulations

To evaluate the overall mechanical performance of the investigated composite formulations, an Integrated Performance Index (IPI) was calculated using five mechanical parameters reported in Table 3: hardness, tensile strength, flexural strength, shear strength, and impact strength. Tensile modulus and flexural modulus were excluded from the analysis to focus the ranking on strength, hardness, and impact resistance. Since the selected parameters have different units and numerical ranges, a maximum-ratio normalization method was employed, as expressed in Eq. 2:

$$N_{ij} = \frac{X_{ij}}{\max_i (X_{ij})} \tag{2}$$

where N_{ij} represents the normalized value of property (j) for composite (i), X_{ij} is the corresponding experimental mean, and $\max_i(X_{ij})$ is the maximum mean value among the investigated formulations (Table 5).

The normalization expressions for the five selected parameters are reported in Table 6.

Equal weights of 0.20 were assigned to all five parameters. The IPI was calculated using Eq. 3:

$$IPI_i = \frac{N_H + N_{TS} + N_{FS} + N_{SS} + N_{IS}}{5} \tag{3}$$

Table 5
Normalization expression.

Hardness (H)	$N_H = \frac{H_i}{84.75}$
Tensile strength (TS)	$N_{TS} = \frac{TS_i}{109.75}$
Flexural strength (FS)	$N_{FS} = \frac{FS_i}{125.50}$
Shear strength (SS)	$N_{SS} = \frac{SS_i}{32.08}$
Impact strength (IS)	$N_{IS} = \frac{IS_i}{20.08}$

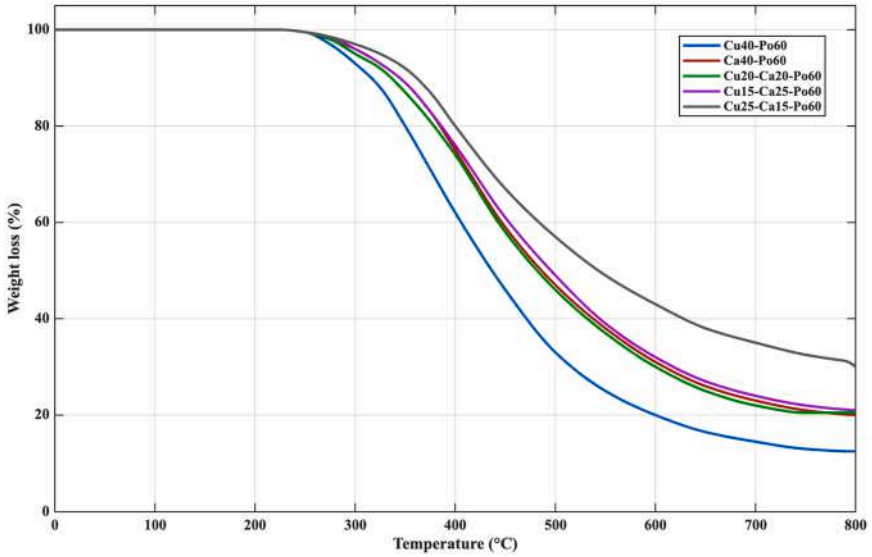

Fig. 21. TGA curve of all tested samples.

Table 6
Normalized mechanical properties, Integrated Performance Index (IPI), and ranking of composite formulations.

Composite formulation	H	TS	FS	SS	IS	IPI	Rank
Cu25-Ca15-Po60	1.000	1.000	1.000	1.000	1.000	1.000	1
Cu15-Ca25-Po60	0.953	0.863	0.896	0.843	0.798	0.871	2
Ca40-Po60	0.870	0.954	0.962	0.935	0.500	0.844	3
Cu20-Ca20-Po60	0.917	0.802	0.837	0.748	0.750	0.811	4
Cu40-Po60	0.710	0.476	0.600	0.437	0.901	0.625	5

It can be clearly seen from the results that Cu25-Ca15-Po60 gave the highest value of IPI, which was equal to 1.0000, whereas the second place was taken by Cu15-Ca25-Po60 (0.8708), followed by Ca40-Po60 (0.8443), Cu20-Ca20-Po60 (0.8106), and Cu40-Po60 (0.6248). The reason for the better position of Cu25-Ca15-Po60 is its maximum hardness (84.75 HRB), tensile strength (109.75 MPa), flexural strength (125.50 MPa), shear strength (32.08 MPa), and impact strength (20.08 J/m). It should be noted that IPI for Cu25-Ca15-Po60 exceeded IPI for carbon and Curauá composites by about 18.4% and 60.1%, respectively. Therefore, the results show that the most suitable composite for the five selected mechanical properties is Cu25-Ca15-Po60.

5. Discussion: quantitative comparison with published studies

Table 7 compares the mechanical, thermal, microstructural, and water absorption characteristics of the developed Curauá–carbon/polyester composites with those reported for natural-fiber and hybrid polymer composites in previous studies. The Cu25-Ca15-Po60 mix-design has achieved tensile and flexural strengths of 109.75 MPa and 125.50 MPa, respectively. Therefore, it clearly demonstrates the beneficial effect of combining Curauá and carbon fibers within a polyester matrix. These strengths exceed those reported by Sharma et al. [32] for alkali-treated Curauá/polypropylene composites (67 ± 2 MPa and 79 ± 1 MPa, respectively). The present tensile strength also exceeds the 34.34 MPa reported by Krishnasamy et al. [81] for the specified Curauá/basalt/polyester configuration, while its flexural strength is comparable to the reported 119.6 MPa. As reported in the literature, relatively higher mechanical strengths were obtained for jute/carbon [60], flax/carbon [84], and other hybrid composites, emphasizing the significance of fiber architecture, amount of reinforcement, matrix material, and stacking pattern. The present hybrid also exhibited reduced water absorption. In thermogravimetric analysis, it was observed that the residual weight of the hybrid composite was 30% at 800 °C under a nitrogen environment, which was higher than 12.5% in the case of the Curauá fiber-reinforced polyester composite (Cu40–Po60), while SEM observations revealed a denser microstructure with fewer voids and signs of fiber pull-out. However, these results indicate a good interaction between fiber and matrix and resistance to water absorption after the hybridization process. However, testing conditions, including testing methods, duration of exposure, orientations of fibers, and polymers matrices do not allow making any comparison of performance among the studies. All reported studies conducted SEM/morphology analysis, and the available information is descriptive; therefore, it is not reported in the comparative table.

6. Conclusion

The mechanical, thermal, and water absorption characteristics of five composite specimens (Cu40-Po60, Ca40-Po60, Cu20-Ca20-Po60,

Table 7
Comparison of the present study with Curauá-based and other natural/synthetic hybrid polymer composites.

Study	Composite / configuration	Tensile properties	Flexural properties	Thermal / TGA	Water absorption
Present study (2026)	Curauá/carbon/polyester (Cu25–Ca15–Po60)	TS 109.75 MPa; TM 5.80 GPa	FS 125.50 MPa; FM 5.50 GPa	~30% residue at 800 °C under N_2; Cu40–Po60: 12.5%	24 h: 2.7% hybrid; 8.2% Cu-only; 1.6% Ca-only
Krishnasamy et al. (2025) [81].	Basalt/Curauá/polyester (75B/25Cu; 8 mm)	TS 34.34 MPa	FS 119.6 MPa	—	—
Sharma et al. (2024) [32]	Alkali-treated Curauá/PP (18 wt% fiber)	TS 67 ± 2 MPa	FS 79 ± 1 MPa	—	—
Costa et al. (2020) [35]	Curauá/GO-functionalized epoxy (CF/GOEM; 30 vol% fiber)	TS + 40%; Young's modulus + 60% relative to CF/EM	—	—	—
Meliande et al. (2022) [42]	Curauá/aramid/epoxy	—	FS −33%; FM −56% with replacement of aramid by Curauá	—	—
Sujon et al. (2020) [60]	Jute/carbon/epoxy (UD)	TS 571 MPa ($J_3C_4J_3$); 496 MPa ($C_2J_6C_2$)	FS 455 MPa ($C_2J_6C_2$)	—	Minimum 3.8% ($C_2J_6C_2$)
Chapman and Dhakal (2019) [84]	Flax/carbon/epoxy	—	FS 95.66 → 425.87 MPa; FM 4.78 → 17.90 GPa	—	—
Wang et al. (2023) [85]	Flax/carbon/FRP (26.4% carbon-fiber volume fraction)	TS + 129.3% relative to flax-only FRP	—	—	—
Yashas Gowda et al. (2022) [86]	Flax/carbon/epoxy (CFFC)	TS 178.48 MPa; TM 2.132 GPa	FS 378.86 MPa; FM 15.76 GPa	Initial degradation 319.29 °C; residue 29.32%	Tested; numerical value omitted
Boccarusso et al. (2023) [87]	Hemp/carbon hybrid laminates (CLC; CHC)	—	CLC: FS 118.9 ± 5.3 MPa; FM 8.30 ± 0.44 GPa. CHC: FS 145.5 ± 6.1 MPa; FM 9.60 ± 0.61 GPa	—	—
Islam et al. (2025a) [45]	Alkali/GO-treated bamboo/epoxy (AGB; 5 mm)	TS 140.23 ± 3.56 MPa; TM 6.11 ± 0.22 GPa	FS 155.62 ± 4.32 MPa; FM 6.03 ± 0.33 GPa	Improved thermal degradation resistance	AGB ~2% equilibrium uptake after ~50 h; test continued to 30 days
Islam et al. (2025b) [46]	GO-treated jute-wrapped glass-core/epoxy (G.cGFJF)	TS 272.63 MPa; TM 7.74 GPa	FS 169.57 MPa; FM 10.42 GPa	—	1.12% GO-treated; 1.81% untreated

Notes: Cu = Curauá fiber; Ca = carbon fiber; B = basalt fiber; Po = polyester resin; PP = polypropylene; FRP = fiber-reinforced polymer; GO = graphene oxide; CF = Curauá fiber (in Costa et al.); EM = epoxy matrix; TS = tensile strength; TM = tensile modulus; FS = flexural strength; FM = flexural modulus; TGA = thermogravimetric analysis; DTG = derivative thermogravimetry; SEM = scanning electron microscopy; UD = unidirectional; CFFC = carbon–flax–flax–carbon laminate; AGB = alkali-treated and graphene oxide-coated bamboo-fiber composite; G.cGFJF = graphene oxide-treated glass-core/jute-wrapped hybrid composite. $J_3C_4J_3$ and $C_2J_6C_2$ indicate stacking sequences, with subscripts representing the number of jute (J) and carbon (C) layers. CLC and CHC denote the carbon/hemp hybrid laminate configurations; wt% = weight percentage; vol% = volume percentage.

Cu15-Ca25-Po60, and Cu25-Ca15-Po60) were evaluated to determine the influence of hybrid fiber reinforcement on the performance of polyester-based composites. Among all samples, Cu25-Ca15-Po60, which contained both Curauá and carbon fibers, exhibited the best overall mechanical properties. It achieved the highest hardness, tensile strength, tensile modulus, flexural strength, flexural modulus, and shear strength, along with superior impact resistance. In contrast, Cu40-Po60, composed solely of Curauá fibers, showed the lowest mechanical performance, confirming the positive effect of hybridization with carbon fibers. The water uptake test revealed that Cu40-Po60 absorbed the most moisture, reaching 8.2% after 24 h, indicating poor resistance to water ingress due to the hydrophilic nature of natural fibers. Conversely, Ca40-Po60 and Cu25-Ca15-Po60 showed significantly lower water absorption values (1.6% and 2.7%, respectively, after 24 h), suggesting that the inclusion of carbon fiber effectively reduced water uptake and enhanced dimensional stability in humid environments. Thermogravimetric analysis (TGA) indicated that all composite specimens retained 100% of their mass up to 75 °C, with thermal degradation initiating gradually beyond this temperature. Cu40-Po60, made solely with Curauá fiber, showed the highest weight loss, ending with only 12.5% residual mass at 800 °C, indicating lower thermal stability. In contrast, Cu25-Ca15-Po60, a hybrid composite with both Curauá and carbon fibers, retained 30% of its mass at the same temperature, demonstrating enhanced thermal resistance. SEM observations aligned with the tensile test results, revealing improved fiber–matrix bonding, reduced voids, and better load transfer in the carbon-reinforced hybrid composite.

The one-way ANOVA results demonstrated that the effect of the composite formulations was significant for all seven mechanical properties ($p < 0.001$) and the maximum F values were found for the shear strength (4329.02) and tensile strength (2376.00). Out of five composite formulations, Cu25-Ca15-Po60 had the highest tensile strength (109.75 MPa) and flexural strength (125.50 MPa), thus, confirming its good mechanical properties. Nevertheless, due to the small number of observations ($n = 4$), these results need further experimental confirmation.

Furthermore, the Integrated Performance Index (IPI), computed by combining five equally weighted mechanical properties, justifies the outstanding mechanical performance of the Cu25-Ca15-Po60 formulation, with the best IPI of 1.0000. This was followed by Cu15-Ca25-Po60 (0.8708), Ca40-Po60 (0.8443), Cu20-Ca20-Po60 (0.8106), and Cu40-Po60 (0.6248). It is clear from the above results that the formulation containing 25% weight of Curauá fiber, 15% weight of carbon fiber, and 60% weight of polyester performs the best in terms of mechanical performance.

Therefore, the results clearly demonstrate that the incorporation of carbon fibers not only improved mechanical strength and stiffness but also contributed to better resistance to moisture absorption and thermal degradation, making hybrid composites like Cu25-Ca15-Po60 highly suitable for structural and environmental applications where both durability and mechanical integrity are essential.

CRediT authorship contribution statement

Karthick Rasu: Writing – review & editing, Writing – original draft, Visualization, Validation, Resources, Methodology, Investigation, Formal analysis, Data curation, Conceptualization. **Arnas Majumder:** Writing – review & editing, Writing – original draft, Visualization, Validation, Software, Resources, Methodology, Investigation, Formal analysis, Data curation, Conceptualization. **Flavio Stochino:** Writing – review & editing, Writing – original draft, Visualization, Validation, Supervision, Software, Resources, Project administration, Methodology, Funding acquisition, Conceptualization.

Declaration of Competing Interest

The authors declare that they have no known competing financial interests or personal relationships that could have appeared to influence the work reported in this paper.

Acknowledgments

The financial support of the PRIN PNRR 2022 - project Integra TRM: Integrated seismic and thermal upgrading of existing masonry buildings through a novel sustainable Textile-Reinforced Mortar system F53D23009850001 is acknowledged. Further, all authors would also like to thank Fondazione di Sardegna: “Thermal and Engineering Response of Recycled Aggregates in Concrete (TERRA)” project (Application No. 10911249) and the RELUIS–DPC 2024–2026 Project, Work Package 5.

Data availability

Data will be made available on request.

References

[1] V. Vignesh, N.B. Karthik Babu, A.M. Arun Mohan, S. Sathees Kumar, N. Nagaprasad, N. Ayrilmis, R. Krishnaraj, Development of hybrid fiber-reinforced vinyl ester composites for civil and automotive applications, Sci. Rep. 15 (2025) 37174, https://doi.org/10.1038/s41598-025-21314-w.

[2] R. Phiri, S. Mavinkere Rangappa, S. Siengchin, Agro-waste for renewable and sustainable green production: A review, J. Clean. Prod. 434 (2024) 139989, https://doi.org/10.1016/j.jclepro.2023.139989.

[3] C. Adarsh, Lalit Ranakoti, Pawan Kumar Rakesh, Niraj Kumar Mishra, Experimental Investigations on Mechanical Properties of Walnut Shell and Pine Needle Ash Polylactic Acid Biocomposites, Compos. Theory Pract. 21 (2021) 114–120.

[4] V. Vignesh, K.A. Balasubramanian, A.M.A. Mohan, S.T.K. Rajan, M.I. Ammarullah, *Hibiscus sabdariffa* L. Fiber (HSF) Rope Mat/Wood Sawdust Filler Polyester Composites for Potential Biomedical Structural Application: Mechanical and Thermal Characteristics, J. Nat. Fibers 23 (2026) 2626509, https://doi.org/10.1080/15440478.2026.2626509.

[5] V. Bahuguna, P.K. Rakesh, A. Mandal, D. Kumar, Characterisation of Gaina cocoon foam: A promising and eco-friendly alternative to synthetic materials, Proc. Inst. Mech. Eng. Part. L J. Mater. Des. Appl. 238 (2024) 1175–1184, https://doi.org/10.1177/14644207231216867.

[6] G. Chinga-Carrasco, J. Ruwoldt, E. Pasquier, M.Ø. Dalheim, M.K. Wieser, Development of a beverage carton closure cap based on 100% wood pulp fibres, J. Clean. Prod. 445 (2024) 141339, https://doi.org/10.1016/j.jclepro.2024.141339.

[7] S.S. Kumar, V.M. Raja, S. Sudhagar, G. Kanagaraj, V. Vignesh, P. Manimaran, Static, Dynamic Mechanical and Thermal Characteristics of Luffa, Morinda tinctoria, and Myrobalan Reinforced Epoxy Hybrid Biocomposites, Fibers Polym. 24 (2023) 2093–2105, https://doi.org/10.1007/s12221-023-00196-7.

[8] J. Wu, Z. Zhao, C. Jiang, Y. Yang, Z. Sun, J. Yuang, F. Xiao, Recent development and application of natural fiber in asphalt pavement, J. Clean. Prod. 449 (2024) 141832, https://doi.org/10.1016/j.jclepro.2024.141832.

[9] R.E. Vera, K.A. Vivas, F. Urdaneta, J. Franco, R. Sun, N. Forfora, R. Frazier, S. Gongora, D. Saloni, L. Fenn, J.Y. Zhu, H. Chang, H. Jameel, R. Gonzalez, Transforming non-wood feedstocks into dissolving pulp via organosolv pulping: An alternative strategy to boost the share of natural fibers in the textile industry, J. Clean. Prod. 429 (2023) 139394, https://doi.org/10.1016/j.jclepro.2023.139394.

[10] Y. Chen, Y. Bi, X. Wu, X. Ding, Impact of additional carbon storage of natural plant fiber on product carbon footprint: A case study of cotton/kapok blended T-shirt VS pure cotton T-shirt, J. Clean. Prod. 434 (2024) 140237, https://doi.org/10.1016/j.jclepro.2023.140237.

[11] G. Rajeshkumar, V. Vignesh, A.M.A. Mohan, S.V.N. Prasaadh, A. Poovarasan, M. I. Ammarullah, Performance Analysis of NaOH-Treated Randomly Oriented *Bauhinia purpurea L* Fiber/Epoxy (BPFE) Composites: Mechanical and Free Vibration Studies for Biomedical Applications, J. Nat. Fibers 22 (2025) 2543119, https://doi.org/10.1080/15440478.2025.2543119.

[12] D. Manikandan, V.C. Sathish Gandhi, R. Kumaravelan, V. Vignesh, Effect of hybrid filler loading (*Polyalthia longifolia* seed and graphite) on the mechanical and thermal properties of vinyl ester composites, Polym. Compos. 45 (2024) 6318–6331, https://doi.org/10.1002/pc.28199.

[13] L. Zhu, B. Chen, J. Liu, S. Chen, Y. Zhang, X. Wang, L. Wang, Assessing baseline water footprints of natural fiber textile products in China, J. Clean. Prod. 379 (2022) 134747, https://doi.org/10.1016/j.jclepro.2022.134747.

[14] A.E. Kabeel, M. Abdelgaied, M.E.H. Attia, M. Arıcı, M.M. Abdel-Aziz, Enhancing the productivity of hemispherical solar distillers using dyed flax fibers as natural inexpensive porous materials, J. Clean. Prod. 379 (2022) 134674, https://doi.org/10.1016/j.jclepro.2022.134674.

[15] J. D.G, V. V, M. Hashem, H. Fouad, Statistical approach to explore sustainable characteristics of cellulosic Desmostachya bipinnata fiber and its chemically

modified conditions, Mater. Res. Express 11 (2024) 095302, https://doi.org/10.1088/2053-1591/ad7446.
[16] I.A.T. Razera, E. Frollini, Composites based on jute fibers and phenolic matrices: Properties of fibers and composites, J. Appl. Polym. Sci. 91 (2004) 1077–1085, https://doi.org/10.1002/app.13224.
[17] L. Prabhu, V. Krishnaraj, S. Sathish, S. Gokulkumar, N. Karthi, L. Rajeshkumar, D. Balaji, N. Vigneshkumar, K.S. Elango, J. Karpagam, V.J. Vijayalakshmi, E. R. Gowarthan, H. Jayakumar, Experimental investigation on mechanical properties of flax/banana/ industrial waste tea leaf fiber reinforced hybrid polymer composites, Mater. Today. Proc. 45 (2021) 8136–8143, https://doi.org/10.1016/j.matpr.2021.02.111.
[18] F. Bollino, V. Giannella, E. Armentani, R. Sepe, Mechanical behavior of chemically-treated hemp fibers reinforced composites subjected to moisture absorption, J. Mater. Res. Technol. 22 (2023) 762–775, https://doi.org/10.1016/j.jmrt.2022.11.152.
[19] H.F.M. de Queiroz, N.V. dos Santos, J.S.S. Neto, M.D. Banea, Mechanical characterization of novel natural fibre-reinforced composites via a three-dimensional fibre architecture, Compos. Sci. Technol. 261 (2025) 110996, https://doi.org/10.1016/j.compscitech.2024.110996.
[20] P.V. Badyankal, T.S. Manjunatha, G.B. Vaggar, K.C. Praveen, Compression and water absorption behaviour of banana and sisal hybrid fiber polymer composites, Mater. Today. Proc. 35 (2021) 383–386, https://doi.org/10.1016/j.matpr.2020.02.695.
[21] R.B. Yusoff, H. Takagi, A.N. Nakagaito, Tensile and flexural properties of polylactic acid-based hybrid green composites reinforced by kenaf, bamboo and coir fibers, Ind. Crops Prod. 94 (2016) 562–573, https://doi.org/10.1016/j.indcrop.2016.09.017.
[22] Z. Alemayehu, R.B. Nallamothu, M. Liben, S.K. Nallamothu, A.K. Nallamothu, Experimental investigation on characteristics of sisal fiber as composite material for light vehicle body applications, Mater. Today. Proc. 38 (2021) 2439–2444, https://doi.org/10.1016/j.matpr.2020.07.386.
[23] G. Ren, B. Yao, M. Ren, X. Gao, Utilization of natural sisal fibers to manufacture eco-friendly ultra-high performance concrete with low autogenous shrinkage, J. Clean. Prod. 332 (2022) 130105, https://doi.org/10.1016/j.jclepro.2021.130105.
[24] K. Rasu, A. Veerabathiran, Performance of high strength natural fiber reinforced hybrid composites for structural engineering applications, Mater. Test. 67 (2025) 553–560, https://doi.org/10.1515/mt-2024-0381.
[25] S. Wasti, D. Kamath, K. Armstrong, C. Clarkson, H. Tekinalp, S. Ozcan, U. Vaidya, Life cycle assessment of coir fiber-reinforced composites for automotive applications, J. Clean. Prod. 485 (2024) 144368, https://doi.org/10.1016/j.jclepro.2024.144368.
[26] A. Figueiredo, G. Vela, G. Ascensão, E. Vettorazzi, R. Vicente, M. Oliveira, Development of an innovative biocomposite using coconut fibres and bio-based binder for thermal and acoustic aplications in buildings, J. Clean. Prod. 491 (2025) 144834, https://doi.org/10.1016/j.jclepro.2025.144834.
[27] G. Venkatesan, V. Vignesh, K.J. Nagarajan, R. Krishnaraj, N. Nagaprasad, K. Vinayagar, Extraction and Characterization of Agricultural Discarded Sesbania Aculeata Stem Waste as Potential Alternate for Synthetic Fibers in Polymer Composites, J. Nat. Fibers 19 (2022) 10601–10615, https://doi.org/10.1080/15440478.2021.2002756.
[28] B. Mano, J.R. Araújo, M.A.S. Spinacé, M.-A.D. Paoli, Polyolefin composites with curaua fibres: Effect of the processing conditions on mechanical properties, morphology and fibres dimensions, Compos. Sci. Technol. 70 (2010) 29–35, https://doi.org/10.1016/j.compscitech.2009.09.002.
[29] J.R. Araujo, B. Mano, G.M. Teixeira, M.A.S. Spinacé, M.-A.D. Paoli, Biomicrofibrilar composites of high density polyethylene reinforced with curauá fibers: Mechanical, interfacial and morphological properties, Compos. Sci. Technol. 70 (2010) 1637–1644, https://doi.org/10.1016/j.compscitech.2010.06.006.
[30] V. Limwibul, P. Jongvivatsakul, T. Jirawattanasomkul, J.-G. Dai, S. Likitlersuang, Bioresin-based composites reinforced with natural fibers and carbon fiber: Mechanical properties and sustainable benefit assessment, J. Mater. Res. Technol. 36 (2025) 140–156, https://doi.org/10.1016/j.jmrt.2025.03.092.
[31] W. de, N.D.R. Martel, I.P. Salgado, F.A.S, The Influence of Fiber Treatment on the Morphology, Water Absorption Capacity and Mechanical Behavior of Curauá Fibers, J. Nat. Fibers 19 (2022) 642–657, https://doi.org/10.1080/15440478.2020.1758863.
[32] A. Sharma, R. Venkatesh, R. Chaturvedi, R. Kumar, P.K.K. Vivekananda, V. Mohanavel, M.E.M. Soudagar, S. Al Obaid, S.H. Salmen, Polypropylene matrix embedded with Curaua fiber through hot compression processing: characteristics study, J. Polym. Res. 31 (2024) 260, https://doi.org/10.1007/s10965-024-04108-y.
[33] L.Q. Minillo, B.C. de, C. Cardoso, A. Ortenzi, Design of nautical cleat for small–medium boats using hybrid curaua–glass fiber–reinforced epoxy, Mater. Today. Proc. 34 (2021) 341–349, https://doi.org/10.1016/j.matpr.2020.06.074.
[34] T. Premkumar, I. Siva, Y. Munde, S. Rajesh, S.C. Amico, Basalt fiber hybridization effects on the thermal degradation properties of curauá fiber composites, Mater. Today. Proc. 28 (2020) 258–260, https://doi.org/10.1016/j.matpr.2020.01.604.
[35] D.O. Castro, A. Ruvolo-Filho, E. Frollini, Materials prepared from biopolyethylene and curaua fibers: Composites from biomass, Polym. Test. 31 (2012) 880–888, https://doi.org/10.1016/j.polymertesting.2012.05.011.
[36] J.R. Araujo, C.B. Adamo, E.D. Robertis, A.Y. Kuznetsov, B.S. Archanjo, B. Fragneaud, C.A. Achete, M.-A.D. Paoli, Crystallinity, oxidation states and morphology of polyaniline coated curauá fibers in polyamide-6 composites, Compos. Sci. Technol. 88 (2013) 106–112, https://doi.org/10.1016/j.compscitech.2013.08.039.
[37] J.H.S. Almeida, S.C. Amico, E.C. Botelho, F.D.R. Amado, Hybridization effect on the mechanical properties of curaua/glass fiber composites, Compos. Part B Eng. 55 (2013) 492–497, https://doi.org/10.1016/j.compositesb.2013.07.014.
[38] M.C. Gutiérrez, M.-A.D. Paoli, M.I. Felisberti, Biocomposites based on cellulose acetate and short curauá fibers: Effect of plasticizers and chemical treatments of the fibers, Compos. Part A Appl. Sci. Manufact. 43 (2012) 1338–1346, https://doi.org/10.1016/j.compositesa.2012.03.006.
[39] U.O. Costa, L.F.C. Nascimento, J.M. Garcia, W.B.A. Bezerra, G.F.F. da Costa, F.S. da Luz, W.A. Pinheiro, S.N. Monteiro, Mechanical properties of composites with graphene oxide functionalization of either epoxy matrix or curaua fiber reinforcement, J. Mater. Res. Technol. 9 (2020) 13390–13401, https://doi.org/10.1016/j.jmrt.2020.09.035.
[40] A.O. da Silva, K.G. de, C. Monsores, S. de, S.A. Oliveira, R.P. Weber, S.N. Monteiro, Ballistic behavior of a hybrid composite reinforced with curaua and aramid fabric subjected to ultraviolet radiation, J. Mater. Res. Technol. 7 (2018) 584–591, https://doi.org/10.1016/j.jmrt.2018.09.004.
[41] U.O. Costa, L.F.C. Nascimento, J.M. Garcia, S.N. Monteiro, F.S.D. Luz, W. A. Pinheiro, F.D.C. Garcia Filho, Effect of Graphene Oxide Coating on Natural Fiber Composite for Multilayered Ballistic Armor, Polymers 11 (2019) 1356, https://doi.org/10.3390/polym11081356.
[42] N.M. Meliande, P.H. Silveira, S.N. Monteiro, L.F. Nascimento, Tensile properties of curaua–aramid hybrid laminated composites for ballistic helmet, Polymers 14 (13) (2022) 2588, https://doi.org/10.3390/polym14132588.
[43] C.C. Angrizani, H.L.O. Júnior, A.J. Zattera, S.C.A, Thermal and Mechanical Investigation of Interlaminate Glass/Curaua Hybrid Polymer Composites (and), J. Nat. Fibers 14 (2017) 271–277, https://doi.org/10.1080/15440478.2016.1193091.
[44] S.N. Monteiro, F.P.D. Lopes, D.C.O. Nascimento, A. da S. Ferreira, K. G. Satyanarayana, Processing and properties of continuous and aligned curaua fibers incorporated polyester composites, J. Mater. Res. Technol. 2 (2013) 2–9, https://doi.org/10.1016/j.jmrt.2013.03.006.
[45] Md.A. Islam, M. Islam, Md.S. Islam, T. Islam, Enhanced properties of bamboo short fiber reinforced polymer composites with alkali and graphene oxide, Mater. Adv. 6 (2025) 4738–4754, https://doi.org/10.1039/D5MA00158G.
[46] M. Islam, M.T. Islam, M.U. Apu, A. Islam, S. Khandaker, F. Sarker, Development of graphene-modified jute/glass hybrid composites *via* fiber wrapping for enhanced structural applications, RSC Adv. 15 (2025) 27594–27605, https://doi.org/10.1039/D5RA02968F.
[47] Md.T. Hossain, S. Reza, Md.A. Islam, Md Mohebbullah, T. Islam, Progress and Prospects of Chemical Functionalization of Textiles Via Nanotechnology, ACS Appl. Eng. Mater. 3 (2025) 1–20, https://doi.org/10.1021/acsaenm.4c00644.
[48] C.O. Nwankwo, J. Mahachi, Bio-Based Polymer Composites Used in the Building Industry: A Review, in: M. Kioumarsi, B. Shafei (Eds.), The 1st International Conference on Net-Zero Built Environment, Springer Nature Switzerland, Cham, 2025, pp. 843–854, https://doi.org/10.1007/978-3-031-69626-8_71.
[49] X.D. Wang, C. Zhang, Z. Huang, G.W. Chen, Impact Experimental Research on Hybrid Bamboo Fiber and Steel Fiber Reinforced Concrete, AMM 357360 (2013) 1049–1052, https://doi.org/10.4028/www.scientific.net/AMM.357-360.1049.
[50] I. Ivanova, J. Assih, C. Diagana, I. Titeux-Peth, Hybrid Composite With Natural and Synthetic Fibers in the Rehabilitation of Reinforced Concrete Structures, Appl. Res. 4 (2025) e202400267, https://doi.org/10.1002/appl.202400267.
[51] J. Qureshi, A Review of Fibre Reinforced Polymer Bridges, Fibers 11 (2023) 40, https://doi.org/10.3390/fib11050040.
[52] R. Chandra Das, A. Ul Islam, S. Dewanjee, T. Akhter, F. Sultana Rafi, S. Mondal, Preparation and Characterization of Aluminium Wire Mat Reinforced Polyester Composite, AMPC 09 (2019) 48–56, https://doi.org/10.4236/ampc.2019.94005.
[53] A. Majumder, F. Stochino, I. Farina, M. Valdes, F. Fraternali, E. Martinelli, Physical and mechanical characteristics of raw jute fibers, threads and diatons, Constr. Build. Mater. 326 (2022) 126903, https://doi.org/10.1016/j.conbuildmat.2022.126903.
[54] N. Saba, M. Jawaid, M.T.H. Sultan, An overview of mechanical and physical testing of composite materials, in: Mechanical and Physical Testing of Biocomposites, Fibre-Reinforced Composites and Hybrid Composites, Elsevier, 2019, pp. 1–12, https://doi.org/10.1016/B978-0-08-102292-4.00001-1.
[55] I.D. Baere, W.V. Paepegem, M. Quaresimin, J. Degrieck, On the tension–tension fatigue behaviour of a carbon reinforced thermoplastic part I: Limitations of the ASTM D3039/D3479 standard, Polym. Test. 30 (2011) 625–632, https://doi.org/10.1016/j.polymertesting.2011.05.004.
[56] K. Yesuraj, R. Sathiyamoorthi, Y. Devarajan, M.D. Babu, N. Kaliappan, A comprehensive experimental study of eco-friendly hybrid polymer composites using pistachio shell powder and Aquilaria agallocha Roxb, Sci. Rep. 14 (2024) 24239, https://doi.org/10.1038/s41598-024-74872-w.
[57] R.T. Haluza, K.L. Koudela, C.E. Bakis, D.O. Adams, J.M. Pereira, Shear Strain Measurement Techniques in Composite V-Notch Shear Testing, Exp. Mech. 62 (2022) 1655–1671, https://doi.org/10.1007/s11340-022-00897-9.
[58] U.O. Costa, L.F.C. Nascimento, J.M. Garcia, W.B.A. Bezerra, S.N. Monteiro, Evaluation of Izod impact and bend properties of epoxy composites reinforced with mallow fibers, J. Mater. Res. Technol. 9 (2020) 373–382, https://doi.org/10.1016/j.jmrt.2019.10.066.
[59] N. Beemkumar, G. Subbiah, V.J. Upadhye, A. Arora, S.P. Jena, K.K. Priya, H. Alemayehu, Thermal stability and flame-retardant properties of a basalt/kevlar fiber-reinforced hybrid polymer composite with bran filler particulates, Results Eng. 25 (2025) 104207, https://doi.org/10.1016/j.rineng.2025.104207.
[60] M.A.S. Sujon, M.A. Habib, M.Z. Abedin, Experimental investigation of the mechanical and water absorption properties on fiber stacking sequence and

orientation of jute/carbon epoxy hybrid composites, J. Mater. Res. Technol. 9 (2020) 10970–10981, https://doi.org/10.1016/j.jmrt.2020.07.079.
[61] G.R. Arpitha, M.J. Raghu, K.N. Bharath, N. Jain, A. Verma, Mechanical and micro-structural characterization of biodegradable coir fiber–glass sheet–charcoal reinforced polymer composite: an experimental approach, Discov. Polym. 1 (2024) 7, https://doi.org/10.1007/s44347-024-00009-x.
[62] G. Velmurugan, J.S. Chohan, R. Maranan, P. Paramasivam, N. Manikandan, P. Thejasree, S.L. Narayana, B.C. Olaiya, M. Kumar, Experimental investigation and optimization of mechanical and tribological performances of bio-based sustainable hybrid composites incorporating Nano-SiO_2 fillers, Sci. Rep. 16 (2026) 7288, https://doi.org/10.1038/s41598-026-38263-7.
[63] S.F. Mansour, S.I. El-dek, M.K. Ahmed, Physico-mechanical and morphological features of zirconia substituted hydroxyapatite nano crystals, Sci. Rep. 7 (2017) 43202, https://doi.org/10.1038/srep43202.
[64] Z. Li, A. Wu, J. Yang, M. Wang, H. Deng, C. Wang, Mechanical properties and design of hybrid composites of carbon and jute fibers with polypropylene, J. Reinf. Plast. Compos. 44 (2025) 1757–1767, https://doi.org/10.1177/07316844241247888.
[65] M.J. John, S. Thomas, Biofibres and biocomposites, Carbohydr. Polym. 71 (2008) 343–364, https://doi.org/10.1016/j.carbpol.2007.05.040.
[66] I.A. Daniyan, K. Mpofu, A.O. Adeodu, O. Adesina, Development of carbon fibre reinforced polymer matrix composites and optimization of the process parameters for railcar applications, Mater. Today. Proc. 38 (2021) 628–634, https://doi.org/10.1016/j.matpr.2020.03.480.
[67] G.G. Del Pino, A. Bezazi, H. Boumediri, A.C. Kieling, C.C. Silva, J. Dehaini, J.L. V. Rivera, M.D.G.D.S. Valenzuela, F.R.V. Díaz, T.H. Panzera, Hybrid epoxy composites made from treated curauá fibres and organophilic clay, J. Compos. Mater. 55 (2021) 57–69, https://doi.org/10.1177/0021998320945785.
[68] S.N. Monteiro, F. Muylaert Margem, N. Tonini Simonassi, R.L. Loiola, M. Picanço Oliveira, Tensile Test of High Strength Thinner Curaua Fiber Reinforced Polyester Matrix Composite, MSF 869 (2016) 361–365, https://doi.org/10.4028/www.scientific.net/MSF.869.361.
[69] H.H.K. Xu, L. Sun, M.D. Weir, S. Takagi, L.C. Chow, B. Hockey, Effects of incorporating nanosized calcium phosphate particles on properties of whisker-reinforced dental composites, J. Biomed. Mater. Res. 81B (2007) 116–125, https://doi.org/10.1002/jbm.b.30644.
[70] M. Jawaid, H.P.S.A. Khalil, Cellulosic/synthetic fibre reinforced polymer hybrid composites: A review, Carbohydr. Polym. 86 (2011) 1–18, https://doi.org/10.1016/j.carbpol.2011.04.043.
[71] J. Zhang, X. Wang, X. Fu, High Mechanic Enhancement of Chopped Carbon Fiber Reinforced-Low-Density Unsaturated Polyester Resin Composite at Low Preparation Temperature with Facile Polymerization, Materials 14 (2021) 4273, https://doi.org/10.3390/ma14154273.
[72] B. Newman, J.D. Randall, R.J. Varley, F. Stojcevski, L.C. Henderson, Bioinspired Hard–Soft Interface Management for Superior Performance in Carbon Fibre Composites, Fibers Polym. 24 (2023) 3279–3288, https://doi.org/10.1007/s12221-023-00265-x.
[73] G. Czél, Development of bi-directional pseudo-ductile glass/carbon-epoxy hybrid composites for improved safety in structural applications, Compos. Part B Eng. 231 (2022) 109546, https://doi.org/10.1016/j.compositesb.2021.109546.
[74] I. Mokhtar, M.Y. Yahya, A.S. Abd Kader, S.A. Hassan, C. Santulli, Transverse impact response of filament wound basalt composite tubes, Compos. Part B Eng. 128 (2017) 134–145, https://doi.org/10.1016/j.compositesb.2017.01.005.
[75] S.S. Kumar, P. Shyamala, P.R. Pati, D.K. Mishra, V. Sharma, G. Tank, M. Kanan, Investigation and machine learning-based prediction of mechanical properties in hybrid natural fiber composites, Sci. Rep. 15 (2025) 33700, https://doi.org/10.1038/s41598-025-18944-5.
[76] A.D.S. Ferreira, F.P.D. Lopes, S.N. Monteiro, K.G. Satyanarayana, Charpy impact resistance of alkali treated curaua reinforced polyester composites, Mat. éria (Rio J. 15 (2010) 131–137, https://doi.org/10.1590/S1517-70762010000200007.
[77] S. Gul, I.E. Tabrizi, B.S. Okan, A. Kefal, M. Yildiz, An experimental investigation on damage mechanisms of thick hybrid composite structures under flexural loading using multi-instrument measurements, Aerosp. Sci. Technol. 117 (2021) 106921, https://doi.org/10.1016/j.ast.2021.106921.
[78] M. Ramesh, C. Deepa, Mechanical properties of natural and synthetic fiber reinforced hybrid composites, in: A. Khan, S.M. Rangappa, S. Siengchin, M. Jawaid, A.M. Asiri (Eds.), Hybrid Natural Fiber Composites, Woodhead Publishing, 2021, pp. 309–325, https://doi.org/10.1016/B978-0-12-819900-8.00013-1.
[79] D.J. Eyckens, C.L. Arnold, J.D. Randall, F. Stojcevski, A. Hendlmeier, M. K. Stanfield, J. Pinson, T.R. Gengenbach, R. Alexander, L.C. Soulsby, P.S. Francis, L.C. Henderson, Fiber with Butterfly Wings: Creating Colored Carbon Fibers with Increased Strength, Adhesion, and Reversible Malleability, ACS Appl. Mater. Interfaces 11 (2019) 41617–41625, https://doi.org/10.1021/acsami.9b11826.
[80] F. Qianqian, C. Li, Effect of thermal bonding layers on interlaminar shear strength of laminated composites, J. Phys. Conf. Ser. 1790 (2021) 012085, https://doi.org/10.1088/1742-6596/1790/1/012085.
[81] S. Krishnasamy, S. Irulappasamy, S.M.K. Thiagamani, R.A. Ilyas, P.S. Khoo, Examining the mechanical properties of hybrid curauá-basalt reinforced polyester composites, Polym. Compos. 46 (2025) 11416–11431, https://doi.org/10.1002/pc.29694.
[82] H. Park, H. Jung, J. Yu, M. Park, S.Y. Kim, Carbon fiber-reinforced plastics based on epoxy resin toughened with core shell rubber impact modifiers, E-Polymers 15 (2015) 369–375, https://doi.org/10.1515/epoly-2015-0068.
[83] K. Hemachandra Reddy, B.M. Reddy, R.M. Reddy, P.V. Reddy, Y.V.M. Reddy, H. R. Rao, Effects of Carbon Fiber Hybridization on Mechanical, Structural, and Thermal Properties of Cordia dichotoma fiber-reinforced epoxy composite, J. Nat. Fibers 20 (2023) 2216950, https://doi.org/10.1080/15440478.2023.2216950.
[84] M. Chapman, H.N. Dhakal, Effects of Hybridisation on the Low Velocity Falling Weight Impact and Flexural Properties of Flax-Carbon/Epoxy Hybrid Composites, Fibers 7 (2019) 95, https://doi.org/10.3390/fib7110095.
[85] A. Wang, X. Liu, Q. Yue, G. Xian, Tensile properties hybrid effect of unidirectional flax/carbon fiber hybrid reinforced polymer composites, J. Mater. Res. Technol. 24 (2023) 1373–1389, https://doi.org/10.1016/j.jmrt.2023.03.078.
[86] Y.G. TG, V. A, M. P, S. Mavinkere Rangappa, S. Siengchin, M. Jawaid, Mechanical and thermal properties of flax/carbon/kevlar based epoxy hybrid composites, Polym. Compos. 43 (8) (2022) 5649–5662, https://doi.org/10.1002/pc.26880.
[87] L. Boccarusso, F. Pinto, K. Myronidis, D. De Fazio, M. Durante, Thin Hybrid Hemp/Carbon Fiber Composites: Manufacturing, Flexural, and Impact Behavior, J. Mater. Eng. Perform. 32 (2023) 3914–3922, https://doi.org/10.1007/s11665-023-07992-5.